

# Antibiotics reduce *Pocillopora* coral-associated bacteria diversity, decrease holobiont oxygen consumption and activate immune gene expression

Michael T. Connelly<sup>1</sup> | Grace Snyder<sup>1</sup> | Ana M. Palacio-Castro<sup>2,3</sup> |  
 Phillip R. Gillette<sup>1</sup> | Andrew C. Baker<sup>1</sup> | Nikki Taylor-Knowles<sup>1</sup>

<sup>1</sup>Department of Marine Biology and Ecology, University of Miami Rosenstiel School of Marine, Atmospheric, and Earth Science, Miami, Florida, USA

<sup>2</sup>University of Miami Cooperative Institute for Marine and Atmospheric Studies, Miami, Florida, USA

<sup>3</sup>Atlantic Oceanographic and Meteorological Laboratory, National Oceanic and Atmospheric Administration, Miami, Florida, USA

#### Correspondence

Nikki Taylor-Knowles, Department of Marine Biology and Ecology, University of Miami Rosenstiel School of Marine, Atmospheric, and Earth Science, 4600 Rickenbacker Causeway, Miami, FL 33149, USA.

Email: [ntraylorknowles@earth.miami.edu](mailto:ntraylorknowles@earth.miami.edu) and [ntraylorknowles@rsmas.miami.edu](mailto:ntraylorknowles@rsmas.miami.edu)

#### Present address

Michael T. Connelly, Department of Invertebrate Zoology, National Museum of Natural History, Smithsonian Institution, Washington, District of Columbia, USA

#### Funding information

2019 RSMAS David Rowland Fellowship

**Handling Editor:** Michael M. Hansen

## Abstract

Corals are important models for understanding invertebrate host-microbe interactions; however, to fully discern mechanisms involved in these relationships, experimental approaches for manipulating coral-bacteria associations are needed. Coral-associated bacteria affect holobiont health via nutrient cycling, metabolic exchanges and pathogen exclusion, yet it is not fully understood how bacterial community shifts affect holobiont health and physiology. In this study, a combination of antibiotics (ampicillin, streptomycin and ciprofloxacin) was used to disrupt the bacterial communities of 14 colonies of the reef framework-building corals *Pocillopora meandrina* and *P. verrucosa*, originally collected from Panama and hosting diverse algal symbionts (family *Symbiodiniaceae*). *Symbiodiniaceae* photochemical efficiencies and holobiont oxygen consumption (as proxies for coral health) were measured throughout a 5-day exposure. Antibiotics altered bacterial community composition and reduced alpha and beta diversity, however, several bacteria persisted, leading to the hypothesis that these bacteria are either antibiotics resistant or occupy internal niches that are shielded from antibiotics. While antibiotics did not affect *Symbiodiniaceae* photochemical efficiency, antibiotics-treated corals had lower oxygen consumption rates. RNAseq revealed that antibiotics increased expression of *Pocillopora* immunity and stress response genes at the expense of cellular maintenance and metabolism functions. Together, these results reveal that antibiotic disruption of corals' native bacteria negatively impacts holobiont health by decreasing oxygen consumption and activating host immunity without directly impairing *Symbiodiniaceae* photosynthesis, underscoring the critical role of coral-associated bacteria in holobiont health. They also provide a baseline for future experiments that manipulate *Pocillopora* corals' symbioses by first reducing the diversity and complexity of coral-associated bacteria.

#### KEY WORDS

antibiotics, bacteria, coral, holobiont, microbiome, transcriptome

This is an open access article under the terms of the [Creative Commons Attribution](#) License, which permits use, distribution and reproduction in any medium, provided the original work is properly cited.

© 2023 The Authors. *Molecular Ecology* published by John Wiley & Sons Ltd.

## 1 | INTRODUCTION

Stony corals in the genus *Pocillopora* (Lamarck 1816) naturally associate with a diverse bacterial community which can contribute to the overall health and adaptive capacity of the coral holobiont (Epstein et al., 2019; Neave et al., 2017; Peixoto et al., 2017; Rosado et al., 2018; van Oppen et al., 2018). Bacterial communities associated with *Pocillopora* corals have been characterized in several studies, where the dominant bacteria belong to the classes Alphaproteobacteria and Gammaproteobacteria within the phylum Proteobacteria (Apprill et al., 2009; Bourne & Munn, 2005; Brener-Raffalli et al., 2018; Ceh et al., 2011; Epstein et al., 2019; Hernández-Zulueta et al., 2016; van Oppen et al., 2018). Overall, certain *Pocillopora*-associated bacteria are hypothesized to enhance cycling of carbon-, nitrogen- and sulphur-containing nutrients within the coral holobiont (Ceh, Kilburn, et al., 2013; Ceh, van Keulen, et al., 2013; Lema et al., 2012; Li et al., 2022) and exclude pathogens via niche occupation, inhibition of quorum sensing and the production of antimicrobial compounds (Ma et al., 2018; Rosado et al., 2018; Song et al., 2018). Other *Pocillopora*-associated bacteria, such as *Vibrio corallilyticus*, have been identified as potential pathogens that can activate virulence factors and infect coral tissues following an environmental cue or trigger (Ben-Haim et al., 2003; Gibbin et al., 2018; Zhou et al., 2019).

One approach to study host-microbe interactions in complex holobionts is to use controlled experiments that aim to manipulate the composition of the host-associated microbiota and reveal the specific microbial processes that contribute to holobiont functions (Chevrette et al., 2019). In idealized model organisms, this involves the elimination of the native microbiota with broad-spectrum antibiotics to produce axenic ("germ-free") or gnotobiotic ("known microbiota") animals that can be used in manipulative experiments to reveal how host-microbe interactions affect the development, physiology and health of the meta-organism (Bosch et al., 2019; Dobson et al., 2016). In axenic or gnotobiotic animals, researchers can investigate the effects of microbial colonization on host immune function, metabolism and gene expression to reveal how specific microbial metabolites interact with host cells and tissues to modulate host physiology and influence the development of various diseases (Kostic et al., 2013; Morgun et al., 2016). To date, no study in corals has achieved this ambitious goal, in part due to coral holobionts' highly complex and tightly associated microbial symbioses among the coral host, *Symbiodiniaceae*, bacterial communities and other viruses and micro-eukaryotes. Despite these limitations (or perhaps because of them), approaches that reduce the diversity and complexity of coral-associated microbiota can yield insights into how these communities affect overall holobiont health and will facilitate future experiments that target specific microbial functions.

In this study, we used high-throughput sequencing and physiological measurements to characterize the effects of antibiotics on 14 colonies of *Pocillopora meandrina* and *P. verrucosa* corals from Panama hosting diverse *Symbiodiniaceae* communities. We hypothesized that antibiotics treatment would (1) reduce coral-associated

bacteria diversity to reveal tightly associated and/or antibiotics-resistant bacteria, (2) cause changes in coral holobiont physiology and metabolism and (3) alter the expression of coral immune genes that mediate host-bacteria interactions. We anticipated that antibiotic suppression of coral bacterial communities would affect coral health and metabolism, symbiotic interactions and immunity and disease resistance and we aimed to measure experimental phenotypes to characterize these changes. Altogether, this study reveals how antibiotic disruption of the coral-associated bacterial community can negatively impact holobiont health and physiology by activating the coral immune response and suppressing net holobiont oxygen consumption and provide a methodological framework that will facilitate future efforts to manipulate corals' symbiotic interactions.

## 2 | MATERIALS AND METHODS

### 2.1 | *Pocillopora* coral colony origins and dominant symbiont types

The 14 *Pocillopora* coral colonies used in the experiment were collected in Panama from Uva Island in the Gulf of Chiriquí and Saboga Island and Urabá Island in the Gulf of Panama on separate trips in 2005, 2010 and 2016 (Figure 1a, Table 1) and maintained in seawater aquaria at the University of Miami until the experiment. *Pocillopora* mitochondrial lineages were assessed by Sanger sequencing the mitochondrial open reading frame (mtORF) using the FATP6.1 and RORF primers (Flot & Tillier, 2007; Flot et al., 2008; Methods S1). Multiple sequence alignment of an 828 bp region used in previous studies was completed using MUSCLE (Edgar, 2004) and haplotype networks were visualized using the R package pegas (Paradis, 2010). Colonies were then assigned to one of the *Pocillopora* mitochondrial lineages in the eastern Pacific (mtORF type 1 [GenBank HQ378758] and type 3 [GenBank HQ378760], sensu [Pinzón et al., 2013; Figure 1b]) and the species names *Pocillopora meandrina* (for mtORF type 1) and *P. verrucosa* (for mtORF type 3) were used according to the most recent *Pocillopora* taxonomy (Gélin et al., 2017; Schmidt-Roach et al., 2014). The dominant symbiont types (*Symbiodiniaceae* genera) in each colony were determined by counting the number of RNAseq reads that aligned against a concatenated reference of the *Symbiodinium*, *Breviolum*, *Cladocopium* and *Durusdinum* genomes (Liu et al., 2018; Shoguchi et al., 2021), using a custom perl script "zooxtype.pl" ([https://github.com/zOnn/2bRAD\\_denovo/blob/master/zooxType.pl](https://github.com/zOnn/2bRAD_denovo/blob/master/zooxType.pl); Wright et al., 2017).

### 2.2 | Antibiotic experimental treatments

*Pocillopora* microfragments were prepared by using stainless steel bone cutters to remove ~5 mm branch tips, which were attached to labelled tags and allowed to recover for 19 days (Methods S1, Figure S1). Microfragments of each colony were assigned to the "baseline," "control" or "antibiotics" treatments, with four

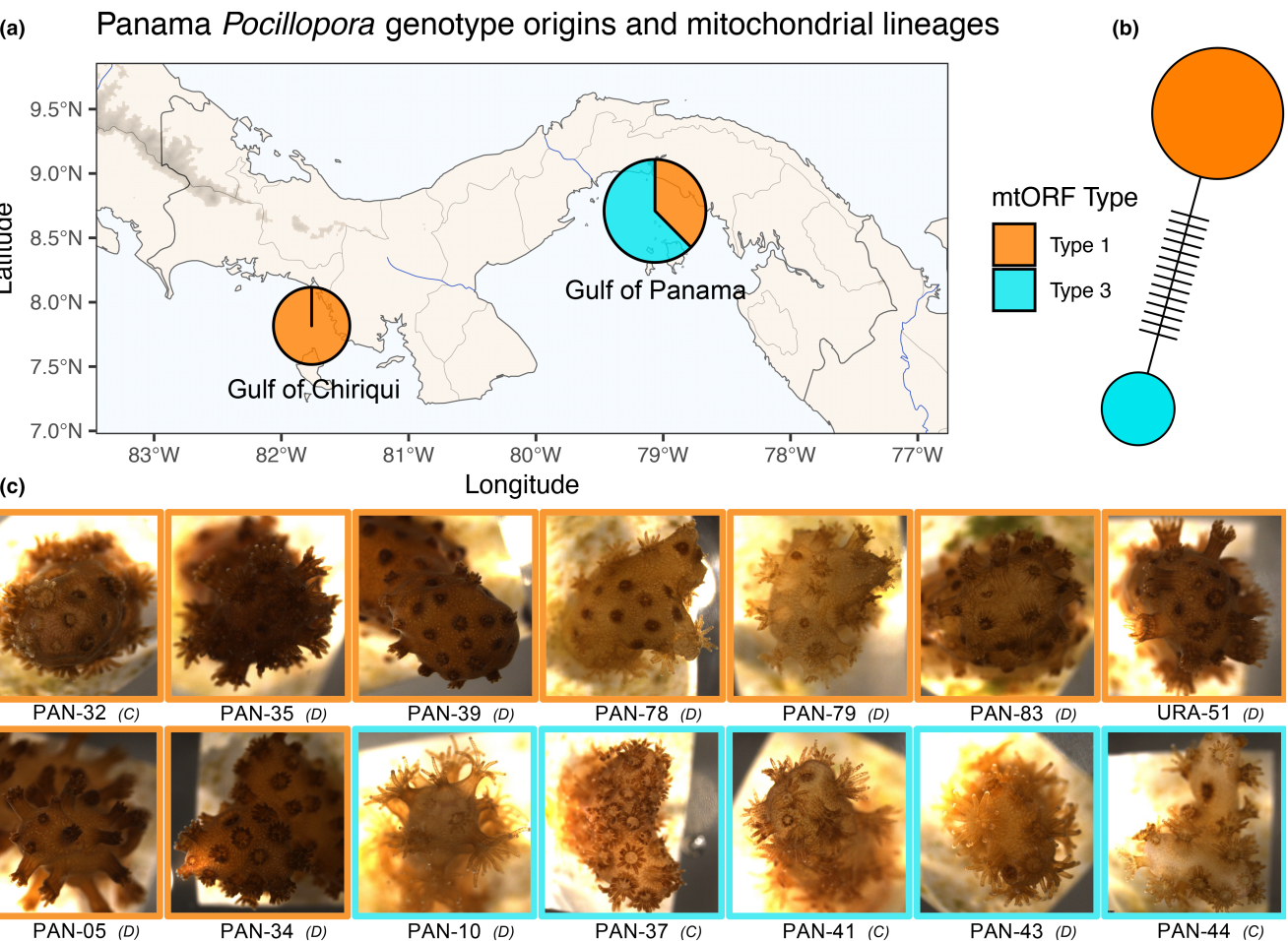


**FIGURE 1** (a) Map of Panama depicting the collection locations of the 14 *Pocillopora* colonies used in the experiment and the proportions of different mtORF types from each location. (b) Haplotype networks of the mtORF region for the *Pocillopora* colonies used in the antibiotics experiment. Two unique haplotypes were detected in an 828-bp alignment, corresponding to *Pocillopora* type 1 (orange) and type 3 (cyan) sensu Pinzón et al. (2013). (c) Representative images of *Pocillopora* microfragments from each colony on the first day of the experiment, outlines are coloured according to mtORF type and dominant symbiont type (C/D) is indicated in parentheses. All colonies in the first row of images were used in transcriptome analyses.

replicates of each colony in each treatment ( $n=168$  total, Figure S1). Microfragments in the baseline treatment were sampled at the start of the experiment and microfragments in the control and antibiotics treatments were kept in 24-well plates, in 3.4 mL wells with 2.5 mL of either filter-sterile seawater (FSW) or antibiotic seawater medium (ASM) consisting of 100 µg/mL ampicillin, 50 µg/mL streptomycin and 10 µg/mL ciprofloxacin in FSW for the 120 h duration of the experiment (Methods S1).

### 2.3 | Coral microfragment physiological measurements

*Symbiodiniaceae* photochemical efficiency was measured as the maximum dark-adapted quantum yield of photosystem II ( $F_v/F_m$ ) using an imaging pulse-amplitude-modulated (I-PAM) fluorometer (Walz GmbH). After 30 min of dark acclimation, images were taken to record microfragment  $F_v/F_m$  values. After a baseline  $F_0$  image,  $F_v/F_m$

values were measured from 24 areas of interest (AOIs) in the images of each of the six plates on each of the 5 days of the experiment.

Microfragment dark oxygen consumption rates were measured using a 24-well microplate respirometer (#SY25040, Loligo Systems) placed in a dark, environmentally controlled room kept at 26°C. Oxygen sensors in 1700 µL wells measured real-time oxygen concentration ( $pO_2$  in % air saturation) every 15 s over 45-min incubations (Figure S2). Microfragment oxygen consumption rates were measured for six plates per day over 4 consecutive days, with 3–6 blank wells to correct for background changes in oxygen concentration (Methods S1; Figure S3).

### 2.4 | Statistical analysis of physiology data

Tests for normality and homogeneity of variances were performed on the *Symbiodiniaceae*  $F_v/F_m$  values. Linear mixed-effect models in the R packages lme4 and lmerTest were used to test for differences

Colony	Location	Gulf	mtORF type	Symbiont genus	Collection year
PAN-05	Saboga	Panama	Type 1	Durusdinium	2005
PAN-10	Saboga	Panama	Type 3	Durusdinium	2005
PAN-39	Saboga	Panama	Type 1	Durusdinium	2016
PAN-37	Saboga	Panama	Type 3	Cladocopium	2016
PAN-41	Saboga	Panama	Type 3	Cladocopium	2016
PAN-43	Saboga	Panama	Type 3	Durusdinium	2016
PAN-44	Saboga	Panama	Type 3	Cladocopium	2016
URA-51	Uraba	Panama	Type 1	Durusdinium	2010
PAN-32	Uva	Chiriquí	Type 1	Cladocopium	2016
PAN-34	Uva	Chiriquí	Type 1	Durusdinium	2016
PAN-35	Uva	Chiriquí	Type 1	Durusdinium	2016
PAN-78	Uva	Chiriquí	Type 1	Durusdinium	2016
PAN-79	Uva	Chiriquí	Type 1	Durusdinium	2016
PAN-83	Uva	Chiriquí	Type 1	Durusdinium	2016

Note: The colonies used in the experiment were chosen to represent the widest possible diversity of *Pocillopora* lineages and host–*Symbiodiniaceae* associations present in the eastern tropical Pacific.

in the photosynthetic efficiencies between different experimental treatments, *Pocillopora* colonies, source locations and dominant symbiont types.

Respirometry data were analysed using the R package respR (Harianto et al., 2019). The analysis of microfragment oxygen consumption rates ( $\text{MO}_2$ ) used oxygen concentration data collected after the initial 15 min of the incubation since microfragments often required this amount of time to equilibrate to conditions on the plate and begin consuming dissolved oxygen at consistent rates. Microfragment  $\text{MO}_2$  was calculated by determining the most linear segment between 15 and 45 min during the incubations using the auto\_resp() function and the final rates were converted into units of nmol  $\text{O}_2/\text{min}$  and corrected, via subtraction, for background respiration in the blank wells.

To test for significant differences in microfragment  $\text{MO}_2$  while accounting for the effect of microfragment mass, a linear regression of  $\log(\text{MO}_2)$  against  $\log(\text{mass})$  was performed and the model residuals were used as the mass-corrected  $\text{MO}_2$  (Figure S4; Drown et al., 2020). Linear mixed-effects models were used to assess the effects of experimental treatment, measurement day and their interaction on microfragment  $F_v/F_m$  values and mass-corrected  $\text{MO}_2$ , with *Pocillopora* mtORF type and dominant symbiont type included in the model as random effects.

## 2.5 | Coral fragment sampling

The experiment ended after 5 days, when microscope observations revealed that a single microfragment in the antibiotics treatment had begun to exhibit signs of coenosarc dissociation and polyp bailout (Figure S5). At the time of sampling, microfragments were preserved in 1.5 mL of 0.2  $\mu\text{m}$  filtered RNA stabilization solution and frozen at -80°C.

**TABLE 1** Summary of *Pocillopora* coral colony traits, including colony ID number, origin location, mtORF type sensu Pinzón et al. (2013) dominant symbiont genus and collection year.

## 2.6 | Sample processing for dual DNA/RNA extractions

Dual DNA/RNA extractions were performed for all coral microfragments ( $n=168$ ) using the ZYMO Quick DNA/RNA MagBead kit (Zymo Research). DNA and RNA concentrations were calculated using the Qubit dsDNA and RNA BR kits respectively (Invitrogen). For sequencing quality control, triplicate extractions were also completed using the ZymoBIOMICS microbial community standard as a positive control and triplicate no-template negative controls were processed using only PCR-grade water.

## 2.7 | Bacterial 16S rRNA gene amplicon sequencing

Bacteria 16S rRNA gene amplicon libraries were created following the Earth Microbiome Project (Gilbert et al., 2014), without pooling triplicate PCR technical replicates (Marotz et al., 2019). The 16S rRNA gene V4 region was amplified using the 515F and 806R primer sets (Apprill et al., 2015). PCR reactions were prepared in a sterile hood and consisted of 20  $\mu\text{L}$  of Platinum Hot Start PCR Master Mix (Thermo Fisher), 1  $\mu\text{L}$  each of the 10  $\mu\text{M}$  forward and reverse primers, 2  $\mu\text{L}$  of template DNA and 26  $\mu\text{L}$  of PCR-grade water for a total reaction volume of 50  $\mu\text{L}$ . Thermocycler conditions consisted of 3 min at 94°C initial denaturation, then 35 PCR cycles of 45 s at 94°C, 60 s at 50°C and 90 s at 72°C followed by a final extension for 10 min at 72°C before holding at 4°C. PCR amplifications were also completed using the ZymoBIOMICS microbial community standard and PCR-grade water as a positive and negative control.

Amplicons were checked for quality and size distribution on a 1.5% TE-agarose gel and DNA concentration was determined using the Qubit dsDNA BR kit (Thermo Fisher). 16S rRNA gene amplicons

from all samples and controls were purified using AMPure XP beads, normalized to 4 nM and pooled before submission to the University of Miami Center for Genome Technology (CGT) for 300 bp paired-end sequencing on the Illumina MiSeq.

## 2.8 | Bacterial community data analysis

Raw 16S rRNA gene sequence reads were processed using QIIME2 version 2020.2 (Bokulich et al., 2018). The plugin q2-demux was used to visualize read quality and DADA2 (Callahan et al., 2016) was used to remove primer sequences, trim poor-quality bases, derePLICATE reads, identify chimeric sequences and merge paired-end reads. q2-feature-table (McDonald et al., 2012) was used to generate sequence summary statistics based on sample metadata. Bacterial 16S rRNA gene sequences were taxonomically classified using q2-feature-classifier (Bokulich et al., 2018) and a Naïve Bayes Classifier previously trained on the SILVA 16S rRNA database (Quast et al., 2013) version 132 QIIME2 release based on the 515F/806RB primer pair (available at <https://data.qiime2.org/2020.2/common/silva-132-99-515-806-nb-classifier.qza>) at the 99% similarity amplicon sequence variant (ASV) level. The plugins q2-alignment (Katoh & Standley, 2013) and q2-phylogeny (Price et al., 2010) were used to create a phylogenetic tree for further downstream analyses and q2-taxa was used to remove all mitochondria and chloroplast sequences from the dataset. Finally, output tables containing ASV counts, phylogenetic trees and sample metadata were exported from QIIME2 and imported into R for statistical analyses.

All bacterial community statistical analyses were conducted in R using the packages phyloseq (McMurdie & Holmes, 2013), vegan (Oksanen et al., 2019), ggplot2 (Wickham, 2016) and the tidyverse (Wickham et al., 2019). All unassigned ASVs and chloroplast and mitochondria ASVs were removed from the dataset and contaminant ASVs in the negative control samples were identified and removed using the R package decontam (Davis et al., 2017). ASV abundances were adjusted with the R package zCompositions before the centred log-ratio (clr) transformation was performed for compositional data analysis (Gloor et al., 2017; Palarea-Albaladejo & Martín-Fernández, 2015). Alpha diversity was calculated using the Chao1 richness, Simpson evenness and Shannon diversity indices and non-parametric Kruskal-Wallis tests were used to test for significant differences between treatments, reef sites and coral colonies (Xia & Sun, 2017; Ziegler et al., 2019). Beta diversity was calculated using Aitchison dissimilarity matrices and visualized using principal components analysis (PCA; Gloor et al., 2017). Permutation tests for homogeneity of multivariate dispersions (PERMDISP) and permutational multivariate analysis of variance (PERMANOVA; Anderson, 2017) were used to test for differences in bacterial community beta diversity between treatments, reef sites and coral colonies. Treatment “core” microbiome ASVs were identified as those present in >75% of samples in the baseline, control or antibiotics treatments using the R package microbiome (Ainsworth et al., 2015; Lahti & Shetty, 2019; Risely, 2020).

## 2.9 | Transcriptome profiling

Transcriptome libraries were prepared using the Lexogen Quantseq 3' mRNA-Seq Library Prep Kit FWD (Lexogen) following manufacturer's instructions. Libraries were submitted for two rounds of sequencing at the University of Miami CGT in December 2020 and June 2021. Libraries were sequenced on the Illumina NovaSeq with 100-bp single-end reads in the first round and 100-bp paired-end reads in the second round, with only forward reads kept for downstream analysis.

## 2.10 | Transcriptome data analysis

Transcriptome data were analysed according to Lexogen recommendations. Raw sequences were checked for quality and adapter dimers using FASTQC (<http://www.bioinformatics.babraham.ac.uk/projects/fastqc/>), poor quality bases and adapters were removed using bbduk ([sourceforge.net/projects/bbmap/](http://sourceforge.net/projects/bbmap/)) and reads were aligned against the *P. damicornis* reference genome using STAR v2.7.9a (Dobin et al., 2013). Reads were quantified at the gene level using featureCounts (Liao et al., 2014). Gene counts were filtered to include only genes with mean counts >3 in at least 90% of samples and counts were normalized using the variance-stabilizing transformation (vst) in the R package DESeq2 (Love et al., 2014). PCA was used to visualize the overall transcriptome patterns and the R package VariancePartition was used to partition total transcriptome variance among explanatory factors including sequencing round, colony, dominant symbiont genus and treatment (Hoffman & Schadt, 2016).

The R package WGCNA (Weighted Gene Co-Expression Analysis, Langfelder & Horvath, 2008) was used to construct a signed co-expression network using vst-normalized gene counts and the bi-weight mid-correlation statistic and a soft-thresholding power of 4. Modules were identified using a cut height of 0.99 and a minimum size of 30 genes and modules with >70% similar expression profiles were merged. Module “eigengene” expression values were correlated against experimental treatments and final  $F_v/F_m$  and MO<sub>2</sub> values to identify significant gene modules ( $p < .05$ ) and highly interconnected module “hub” genes were identified within each module. Functional enrichment tests of euKaryotic Orthologous Group (KOG) and Gene Ontology (GO) terms were performed for DEG sets and co-expressed gene modules using the R packages KOGMWU and GO\_MWU (Barfield et al., 2018; Matz, 2019; Wright et al., 2017).

All scripts used in physiology, microbiome and transcriptome data analysis are available at: [https://github.com/michaelconnelly/coral\\_antibiotics\\_physiology](https://github.com/michaelconnelly/coral_antibiotics_physiology).

## 3 | RESULTS

### 3.1 | *Pocillopora* colony mtORF type and *Symbiodiniaceae* diversity

Fourteen *Pocillopora* colonies were used for microfragment preparation and colony traits are summarized in Table 1. Six colonies were

from the Gulf of Chiriquí and eight colonies were from the Gulf of Panama while nine colonies belonged to mtORF type 1 (*P. mean-drina*) and five colonies belonged to mtORF type 3 (*P. verrucosa*, Figure 1b,c). According to RNAseq read alignments, four colonies were dominated by *Cladocopium* and 10 colonies were dominated by *Durusdinium* (Table 1, Figure S6). Microfragment masses ranged from 0.08 to 3.60 g ( $0.148 \pm 0.058$  g, mean  $\pm$  SD).

### 3.2 | Antibiotics treatment does not affect *Symbiodiniaceae* photosynthetic efficiency

Over the 5-day experiment, 560  $F_v/F_m$  measurements were obtained for 112 coral microfragments in the control and antibiotics treatments and all 160 blank measurements returned  $F_v/F_m$  values of 0. Linear mixed-effect models for effects of treatment and measurement day that included *Pocillopora* colony, mtORF type and dominant symbiont genus as random effects revealed that antibiotics treatment had no significant effect on symbiont  $F_v/F_m$  values ( $F=2.72$ ,  $df=1$ ,  $p>.05$ ), despite a significant effect of measurement day ( $F=7.12$ ,  $df=4$ ,  $p<.01$ ). *Pocillopora* mtORF type and dominant symbiont genus were significant random effects ( $p<.01$ , Table S1), with colonies with mtORF type 1 having higher  $F_v/F_m$  values than colonies with mtORF type 3 and colonies hosting *Cladocopium* having higher  $F_v/F_m$  values than colonies hosting *Durusdinium* (Figure 2a). The significant difference in  $F_v/F_m$  values between days was attributed to a significant decline in  $F_v/F_m$  values on Day 2 that recovered as the experiment continued (Figure 2a).

### 3.3 | Antibiotics treatment significantly decreases *Pocillopora* microfragment oxygen consumption

*Pocillopora* microfragment  $MO_2$  rates across all measurements obtained in the experiment ranged between 0.13 and 4.77 nmol  $O_2$ /min ( $1.35 \pm 6.75 \times 10^{-4}$ , mean  $\pm$  SD; Figure 2b). The linear regression model of  $\log(MO_2)$  against  $\log(\text{mass})$  ( $y=-2.41+0.61x$ ,  $R^2=.15$ ,  $N=448$ ) enabled the calculation of mass-corrected  $MO_2$  values (Figure S4). Linear mixed-effect models detected a significant effect of antibiotics treatment on mass-corrected  $MO_2$  values ( $F=71.24$ ,  $df=1$ ,  $p<.001$ ) with lower  $MO_2$  values for antibiotics treatment samples compared to control samples and no significant effect of measurement day ( $F=0.25$ ,  $df=4$ ,  $p>0.1$ ). Neither mtORF type nor symbiont genus showed significant random effects ( $p>0.1$ ; Table S1).

### 3.4 | 16S rRNA gene amplicon sequencing results

16S rRNA gene V4 amplicon sequencing yielded 19.5 million reads, with 4831–428,372 reads per sample ( $106,245 \pm 58,090$ , mean  $\pm$  SD) across all samples in the baseline ( $n=54$ ), control

( $n=56$ ) and antibiotics ( $n=56$ ) treatments (Figure S7). Two baseline samples were removed for low read depth (<1000 reads). The R package decontam identified nine contaminant ASVs with higher abundances in the negative controls than all other samples. After the removal of contaminant sequences and 309 unassigned, chloroplast and mitochondrial sequences from the dataset, a total of 1835 ASVs remained for analyses of bacterial community diversity and composition.

### 3.5 | Antibiotics treatment alters *Pocillopora*-associated bacterial community composition and reduces diversity

Principal components analysis of clr-transformed bacteria abundances revealed that coral samples in the antibiotics treatment clustered separately from baseline and control samples along PC1, which explained 45.3% of the variance and PC2, which explained 6.0% of the variance (Figure 3a). PERMDISP tests rejected the null hypothesis of no differences in dispersion between treatments ( $F=15.92$ ,  $p<.001$ ) and PERMANOVA tests accordingly revealed that samples in the antibiotics treatment had significantly different bacterial communities from baseline and control samples ( $F=17.041$ ,  $p<.001$ ), with no significant differences between the baseline and control treatments. PERMDISP and PERMANOVA tests also revealed no significant differences in bacterial communities due to *Pocillopora* colony, mtORF type, dominant symbiont genus or source location ( $p>.05$ ).

Non-parametric Kruskal-Wallis tests revealed significant differences in alpha-diversity metrics between treatments, including the number of observed ASVs (Kruskal-Wallis chi-squared = 100.35,  $df=2$ ,  $p<.001$ ), Chao1 (Kruskal-Wallis chi-squared = 100.35,  $df=2$ ,  $p<.001$ ) and Shannon's (Kruskal-Wallis chi-squared = 76.54,  $df=2$ ,  $p<.001$ ) and Simpson's (Kruskal-Wallis chi-squared = 63.30,  $df=2$ ,  $p<.001$ ) diversity indices (Figure 3b). Significant decreases in alpha diversity were observed in antibiotics treatment samples, with the average number of ASVs declining 60.5% from  $130 \pm 41.42$  (mean  $\pm$  SD) in baseline samples and  $126.77 \pm 41.18$  in control samples to  $51.34 \pm 18.46$  in antibiotics treatment samples (Figure 3b). Furthermore, Kruskal-Wallis tests revealed significant differences in bacterial community beta diversity between treatments as measured by the distances to centroids (Kruskal-Wallis chi-squared = 34.85,  $df=2$ ,  $p<.001$ ; Figure 3c), indicating reduced community dissimilarity among antibiotics-treated samples relative to baseline and control samples.

### 3.6 | Effects of antibiotics treatment on specific *Pocillopora*-associated bacterial taxa

The bacterial community compositions of the baseline and control samples were similar, with both groups dominated by bacteria in

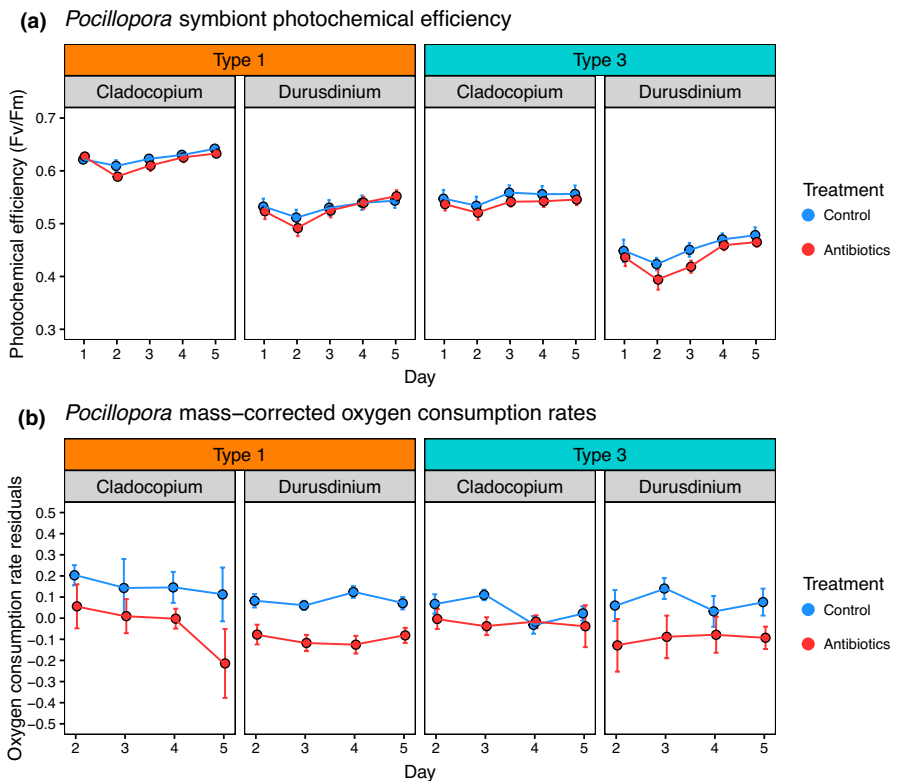


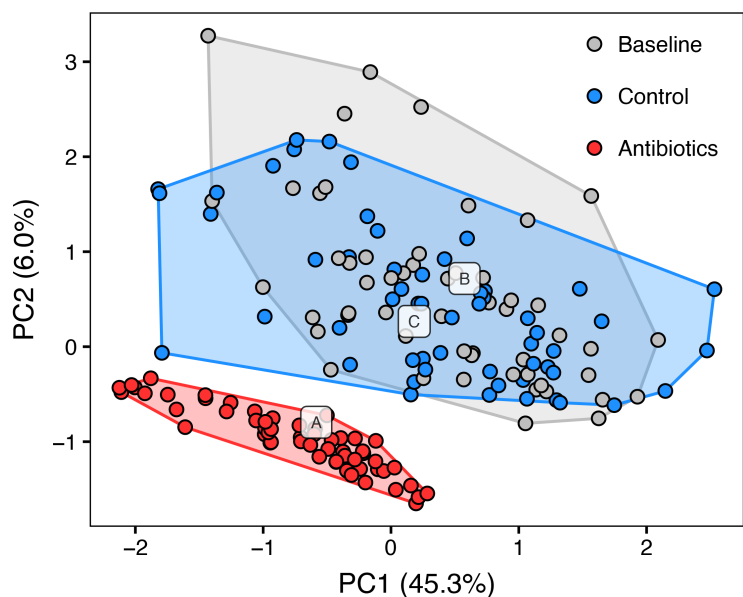
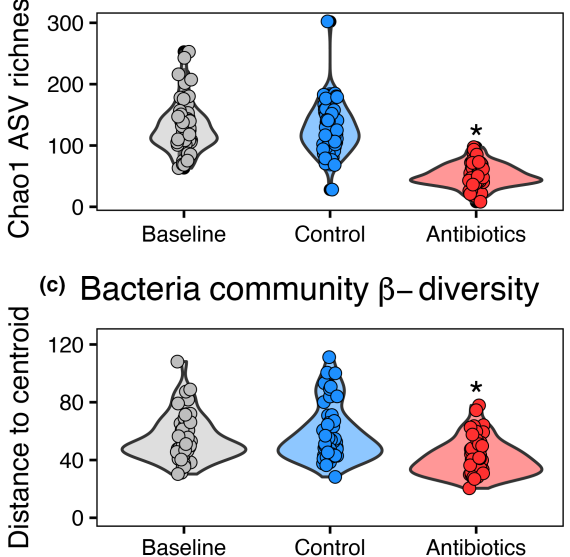
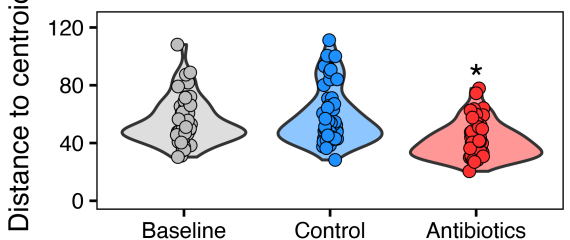
**FIGURE 2** Antibiotics effect on *Pocillopora* coral physiology. (a)  $F_v/F_m$  values for *Pocillopora* coral microfragments in the control and antibiotics treatments throughout the 5-day experiment reveal no effect of antibiotics treatment and significant effects of dominant symbiont genus and measurement day. Average  $F_v/F_m$  values are plotted with error bars representing standard error of the mean. (b) Average mass-corrected oxygen consumption values for *Pocillopora* microfragments in the control and antibiotics treatments from Day 2 to Day 5 of the experiment reveal decreased oxygen consumption in antibiotics-treated microfragments. Average mass-corrected  $\text{MO}_2$  values are plotted with error bars representing standard error of the mean. Mass-corrected  $\text{MO}_2$  values were significantly different between the control and antibiotics treatments, with antibiotics-treated fragments displaying lower rates.

the phylum Proteobacteria (~79%), with lower relative abundances of the phyla Desulfobacterota (6.2%), Acidobacteriota (3.5%), Planctomycetota (3.5%), Bacteroidota (3.3%) and Campilobacterota (2.5%). The 10 most abundant bacterial families in the baseline and control samples were Nitrincolaceae (11.3%), Rhodobacteraceae (7.3%), Thalassospiraceae (6.4%), Cellvibrionaceae (6.1%), Magnetospiraceae (5.8%), Alteromonadaceae (4.6%), Stappiaceae (4.3%), Vibrionaceae (4.1%), Desulfobacteraceae (4.0%) and Methyloligellaceae (3.9%) (Figure S8).

Changes in the bacterial communities of antibiotics-treated samples were driven by dramatic reductions in the relative abundance of several taxa, such as the family Nitrincolaceae, which was reduced from 15.5% in baseline samples and 7.4% in control treatment samples to <0.1% abundance in the antibiotics-treated samples (Figure 3d, Figure S8). Similarly, bacteria in the family Rhodobacteraceae were reduced from 8.4% and 6.3% in the baseline and control samples to 0.3% in antibiotics-treated samples and bacteria in the family Alteromonadaceae were reduced from 5.6% and 3.7% in the baseline and control samples to <0.1% relative abundance in antibiotics-treated samples (Figure 3d, Figure S8), indicating high susceptibility to the chosen antibiotics. Antibiotics treatment samples were dominated by bacteria in the phyla Proteobacteria (58.7%),

Desulfobacterota (18.3%) and Planctomycetota (12.5%), with lower abundances of Campilobacterota (4.4%), Myxococcota (2.8%) and Bacteroidota (1.1%). The most abundant families in antibiotics-treated samples were Vibrionaceae (19.5%), Desulfobacteraceae (16.6%), Endozooicomonadaceae (9.7%), Pirellulaceae (5.7%), Micavibrionaceae (5.5%), Phycisphaeraceae (4.9%), Magnetospiraceae (4.7%), Arcobacteraceae (4.4%) and Methyloligellaceae (4.0%), with lower abundances of the families Thalassospiraceae (3.9%), Myxococcaceae (2.7%) and Kordiimonadaceae (2.7%) (Figure 3d, Figure S8).

To determine specific ASVs driving differences between treatments, “core” microbiomes were identified separately for each treatment as ASVs with >75% prevalence in the baseline ( $n=48$ ), control ( $n=40$ ) or antibiotics ( $n=14$ ) treatments. A total of 54 ASVs were present across all treatment core microbiomes (Figure 3d, Tables S2–S4). There were 27 ASVs shared between the baseline and control core microbiomes that were eliminated from the core microbiome of the antibiotics-treated samples, including three ASVs in the family Rhodobacteraceae and two ASVs in each of the genera *Neptuniibacter*, *Kordiimonas*, *Labrenzia* and *Magnetospira* (Figure 3d, Table S5). Conversely, 10 ASVs shared between the baseline and control treatment core microbiomes persisted into the

(a) *Pocillopora* bacterial communities PCA(b) Bacteria community  $\alpha$ -diversity(c) Bacteria community  $\beta$ -diversity

(d) Treatment core ASVs (e) Relative abundances of all treatment core ASVs

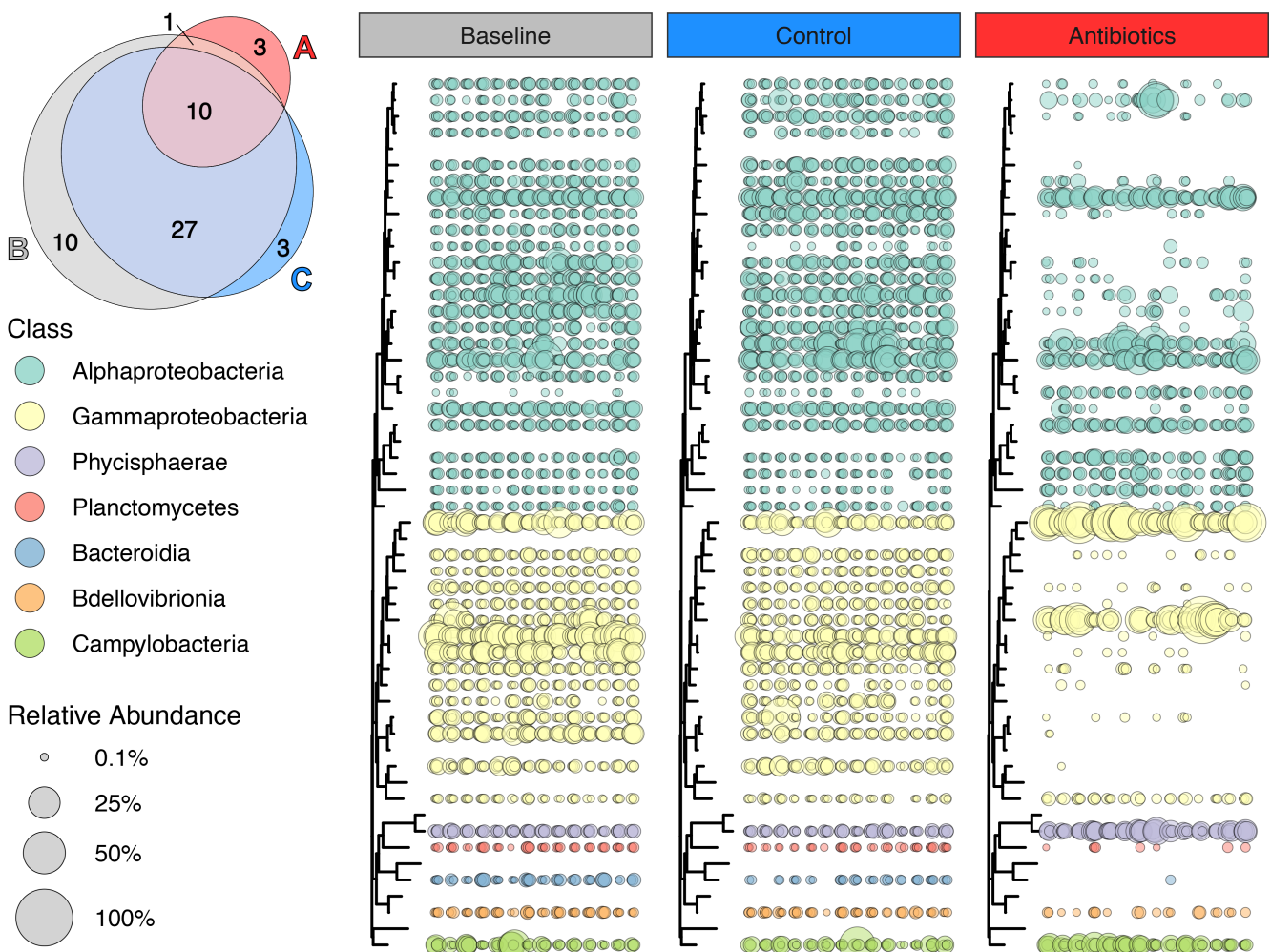


**FIGURE 3** Antibiotics effect on *Pocillopora* coral-associated bacteria community composition, diversity and core microbiome taxa. (a) Principal components analysis (PCA) plot of *Pocillopora* bacterial communities in the baseline, control and antibiotics treatments reveals that antibiotics samples cluster separately from baseline and control samples and have a narrower distribution along the first two PC axes. Baseline samples are coloured grey, control samples are coloured blue and antibiotics samples are coloured red. Convex hull polygons for each treatment show a clear separation of antibiotics-treated samples, whereas baseline and control samples overlap in their distribution. Violin plots of bacterial community (b) alpha diversity and (c) beta diversity show that bacterial community diversity is significantly reduced in the antibiotics treatment. Alpha diversity is represented as the Chao1 metric and beta diversity is represented as the distance to treatment centroid using the Aitchinson distance PCA. (d) Area proportional Euler diagram of treatment “core” (>75% prevalence across samples) identifies unique and shared bacterial amplicon sequence variants (ASVs) across treatments. (e) Bubble plot of the relative abundances of all treatment core ASVs ( $n=54$  total) reveals that bacterial community shifts in the antibiotics treatment are driven by depletion of 27 ASVs and persistence of 10 ASVs.

antibiotics treatment core microbiome (Figure 3d, Table S6). These consisted of one ASV in the genus *Endozooicomonas*, one ASV in the genus *Vibrio*, three ASVs in the family *Micavibrionaceae* and one ASV each in the genus *Thalassospira* and families *Phycisphaeraceae*, *Magnetospiraceae*, *Arcobacteraceae* and *Methyloligellaceae* (Table S6).

### 3.7 | Transcriptome sequencing results

Transcriptome sequencing succeeded for 101 samples in total, with 60 and 41 in each round. Of these, 53 samples from 7 colonies (PAN-32, PAN-35, PAN-39, PAN-78, PAN-79, PAN-83 and URA-51, all *P. meandrina*, mtORF type 1) were used in downstream transcriptome analyses because each colony had at least three replicate samples in both the control and antibiotics treatments. RNAseq of these 53 samples yielded approximately 915.1 million raw reads ranging from 3.3 to 24.8 million reads per sample ( $17.3 \pm 5.5$  million, mean  $\pm$  SD) and 44.9% of total reads aligned to the *P. damicornis* genome (Figure S9). Filtering only genes with mean counts  $>3$  in at least 90% of samples left 17,144 *Pocillopora* genes remaining for downstream expression analyses.

Principal components analysis visualization and Variance Partition analysis of vst-normalized gene counts indicated that *Pocillopora* colony accounted for the most variance in overall gene expression, followed by dominant symbiont type and treatment (Figure 4a,b, Figure S10). However, PERMANOVA tests revealed significant differences in overall gene expression profiles between control and antibiotics-treated samples ( $F=2.156$ ,  $p<.01$ ), between colonies with different dominant symbiont types ( $F=3.153$ ,  $p<.01$ ) and among different individual colonies ( $F=2.539$ ,  $p<.01$ ). Tests for differential gene expression in the overall model between the antibiotics and control treatment revealed 1154 DEGs (776 up, 378 down, Table S7). Top upregulated BP GO terms included “protein folding,” “receptor-mediated endocytosis,” “Golgi vesicle transport,” “response to topologically incorrect protein” and “antigen processing and presentation,” while top downregulated BP GO terms included “gamma-aminobutyric acid metabolic process,” “nitrogen utilization,” “dopaminergic synaptic transmission,” “serine transport,” “tertiary alcohol metabolic process” and “branched-chain amino acid transport” (Figure 4c, Table S8).

### 3.8 | WGCNA identifies co-expressed gene modules correlated with antibiotics treatment and physiology metrics

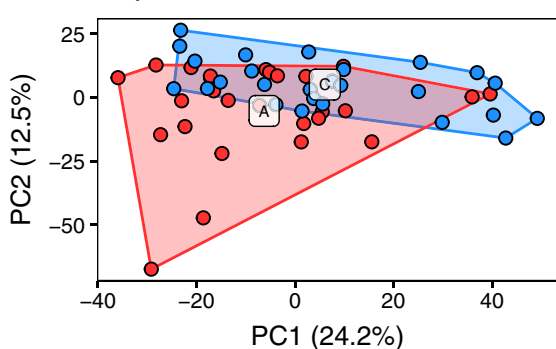
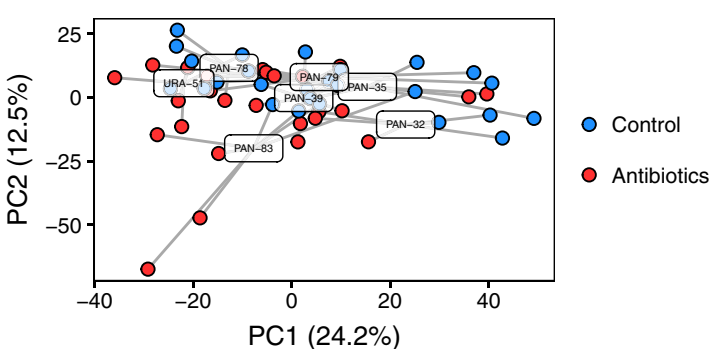
Weighted Gene Co-Expression Analysis identified 17 gene co-expression modules that contained 42–4096 genes and were labelled according to module size along a standard sequence of colours within the WGCNA R package (Figure S11). Module eigengenes of 12 modules were significantly correlated ( $p<.05$ ) with one or more treatments or physiology metrics and six modules were significantly enriched for one or more KOG terms (Figure 5, Table S10).

The “brown” module ( $n=2869$  genes) was the most negatively correlated with the antibiotics treatment and most positively correlated with the control treatment and final  $\text{MO}_2$  values (Figure 5). The “brown” module was enriched for the KOG terms “cytoskeleton,” “transcription,” “RNA processing and modification,” “chromatin structure and dynamics” and “cell cycle control,” and was also enriched for BP GO terms ( $n=236$ ,  $p_{\text{adj}}<.05$ ), including “negative regulation of transcription,” “DNA packaging,” “RNA processing,” “intracellular mRNA localization,” “negative regulation of organelle organization,” “dendrite development,” “epigenetic regulation of gene expression” and “regulation of cell morphogenesis.” The module hub gene was similar to probable global transcription activator SNF2L1 (Smarca1, pdam\_00020473) (Table S9) and other highly connected genes ( $kME>0.7$ ) included collagen alpha-chain (Col6a4, pdam\_00011689), cytoskeleton-associated protein 5 (CKAP5, pdam\_00005151), titin (TTN, pdam\_00005990) and microtubule actin cross-linking factor 1 (MACF1, pdam\_00009389).

Conversely, the “lightyellow” module ( $n=4096$  genes) was the most positively correlated with the antibiotics treatment and most negatively correlated with the control treatment. The “lightyellow” module was enriched for the KOG term “signal transduction mechanisms” and the BP GO terms ( $n=132$ ,  $p_{\text{adj}}<.05$ ) “regulation of cell activation,” “calcium ion transmembrane transport,” “G protein-coupled receptor signaling pathway,” “activation of adenylyl cyclase activity,” “positive regulation of interleukin-6 production” and “regulation of ERK1 and ERK2 cascade.” The module hub gene (pdam\_00021164) and 11 other top-connected genes ( $kME>0.9$ ) had no matches to any proteins in the UniProt database (Table S9), however, other highly connected genes were similar to pentraxin-4 (PTX4, pdam\_00021627), protein decapentaplegic

*Pocillopora* transcriptome PCA

## (a) Experimental treatment

(b) *Pocillopora* genotype

## (c) GO terms enriched in antibiotics treatment DEGs

 $p < 1e-05$  $p < .001$  $p < .01$ 

## BP

0/14 proteasomal ubiquitin-independent protein catabolic process  
26/133 protein polyubiquitination  
9/45 regulation of cellular amino acid metabolic process  
35/119 antigen processing and presentation  
20/70 antigen processing and presentation of peptide antigen via MHC class I  
8/32 proteasome assembly  
20/62 ubiquitin-dependent ERAD pathway  
**48/211 proteasomal protein catabolic process**  
131/651 cellular macromolecule catabolic process  
117/518 protein catabolic process  
10/29 protein quality control for misfolded or incompletely synthesized proteins  
164/689 protein folding  
29/84 protein N-linked glycosylation  
27/118 tRNA metabolic process  
157/850 RNA processing  
100/477 amide biosynthetic process  
15/38 cytoplasmic translational initiation  
16/41 'de novo' protein folding  
**49/156 protein folding**  
13/33 chaperone-mediated protein folding  
5/19 protein refolding  
19/58 regulation of nuclease  
**50/132 response to topologically incorrect protein**  
56/171 response to endoplasmic reticulum stress  
17/70 protein transmembrane transport  
184/737 intracellular protein transport  
5/20 protein import into mitochondrial matrix  
3/164 mitochondrial transport  
**17/65 protein localization to mitochondrion**  
9/22 protein insertion into mitochondrial membrane  
13/38 protein insertion into membrane  
6/59 mitochondrial translation  
**59/330 mitochondrial organization**  
69/199 vesicle organization  
**27/71 vesicle budding from membrane**  
10/16 COP1-coated vesicle budding  
16/30 Golgi vesicle budding  
23/46 vesicle targeting  
**84/250 Golgi vesicle transport**  
**42/109 endoplasmic reticulum to Golgi vesicle-mediated transport**  
7/12 COP1-coated vesicle budding  
20/39 retrograde vesicle-mediated transport, Golgi to endoplasmic reticulum  
5/8 positive regulation of Wnt protein secretion  
17/40 intra-Golgi vesicle-mediated transport  
21/49 retrograde transport, endosome to Golgi  
12/31 proton transmembrane transport  
9/18 energy coupled proton transmembrane transport, against electrochemical gradient  
**138/637 receptor-mediated endocytosis**  
131/587 response to wounding  
25/103 epidermal growth factor receptor signaling pathway  
17/149 taxis  
13/52 actin filament-based movement  
40/175 muscle system process  
22/78 positive regulation of transmembrane transport  
7/133 regulation of ion transport  
5/205 regulation of membrane potential  
29/147 action potential  
32/122 sensory perception of light stimulus  
4/8 gamma-aminobutyric acid metabolic process  
147/560 brain development  
15/69 mechanoreceptor differentiation  
25/151 cell adhesion  
102/413 biological adhesion  
13/98 cell-cell adhesion via plasma-membrane adhesion molecules  
42/130 drug transport  
19/45 drug transmembrane transport  
9/36 chloride transport  
79/316 anion transport  
**22/76 inorganic anion transport**  
17/86 sodium ion transport  
18/91 response to calcium ion  
17/84 digestion  
27/123 cellular response to xenobiotic stimulus  
10/36 non-recombinational repair

## MF

30/172 catalytic, acting on DNA  
9/48 damaged DNA binding  
12/49 phosphoric diester hydrolase  
48/214 regulatory region nucleic acid binding  
23/84 cis-regulatory region binding  
20/79 obsolete protein transporter  
9/30 macromolecule transmembrane transporter  
16/44 GDP binding  
61/224 guanyl nucleotide binding  
17/67 ribonucleoprotein complex binding  
6/10 7S RNA binding  
28/95 translation regulator  
20/60 translation factor, RNA binding  
110/592 RNA binding  
6/31 tRNA binding  
8/19 ATPase regulator  
**21/84 unfolded protein binding**  
52/211 anion transmembrane transporter  
6/22 dicarboxylic acid transmembrane transporter  
5/8 L-serine transmembrane transporter  
11/38 chloride transmembrane transporter  
13/59 inorganic anion transmembrane transporter  
15/73 sodium ion transmembrane transporter  
53/217 channel  
21/80 voltage-gated channel  
55/340 signaling receptor  
15/51 ATPase-coupled ion transmembrane transporter  
29/103 primary active transmembrane transporter  
9/18 ATPase, coupled to transmembrane movement of ions, rotational mechanism  
18/67 proton transmembrane transporter  
10/28 pyrophosphate hydrolysis-driven proton transmembrane transporter  
22/75 actin filament binding  
94/435 cytoskeletal protein binding  
14/24 SNAP receptor  
4/14 fatty acid derivative binding

**FIGURE 4** Principal components analysis (PCA) plot of *Pocillopora* coral gene expression showing the effects of (a) antibiotics treatment and (b) coral genotypic variation on overall transcriptome patterns; control samples are coloured blue and antibiotics samples are coloured red. (c) Biological process (BP) and molecular function (MF) GO terms that were significantly enriched in the DEGs identified in the overall model between the antibiotics treatment and control treatment; upregulated GO terms are red and downregulated GO terms are blue.

## WGCNA module correlation heatmap and KOG enrichment scores

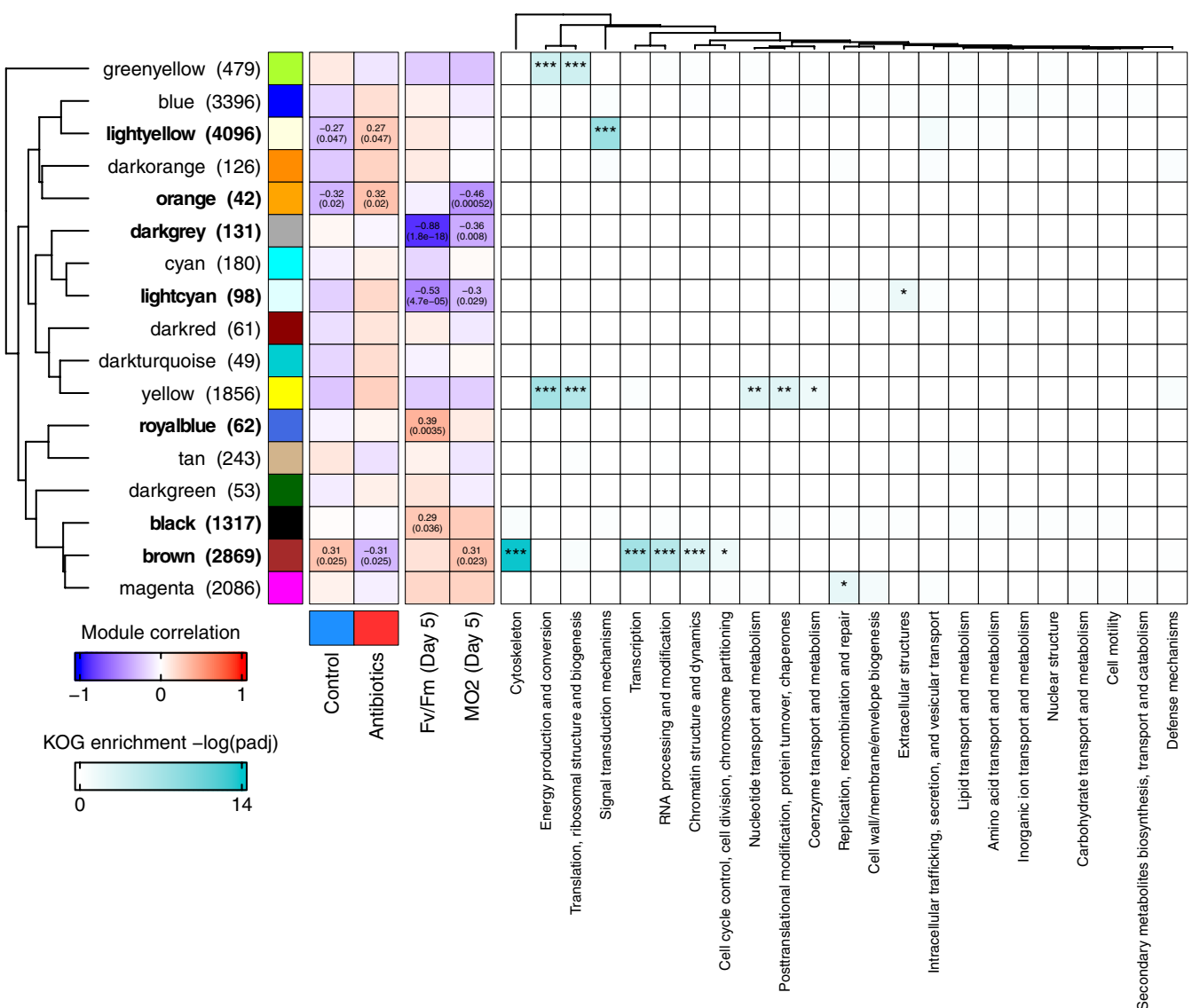


**FIGURE 5** Weighted Gene Co-Expression Analysis module correlation heatmap reveals *Pocillopora* co-expressed gene modules are correlated with treatment responses and physiological metrics and enriched for KOG terms representing key biological processes. Significant treatment and physiology-correlated modules are listed in bold and module correlation coefficients and *p*-values are shown in the heatmap cells. Significantly enriched KOG terms for each module are marked with asterisks (\*\**p* < .001, \*\**p* < .01, \**p* < .05).

(dpp, pdam\_00000055), visual pigment-like receptor peropsin (RRH, pdam\_00020859), sushi, von Willebrand factor type A, EGF and pentraxin domain-containing protein 1 (SVEP1, pdam\_00009413), gamma-glutamyl peptidase 3 (GGP3, pdam\_00013248) and a CuZn-superoxide dismutase (SODCP, pdam\_00019857).

The “orange” module (*n*=42 genes) was also positively correlated with the antibiotics treatment and negatively correlated with the control treatment and negatively correlated with final MO<sub>2</sub> values, but had no significantly enriched KOG or GO terms. While module hub gene (pdam\_00017535) had no matches to any proteins in the UniProt database (Table S9), the other top-connected genes were similar to X-box-binding protein 1 (pdam\_00016926) and prothrombin, or coagulation factor II (F2, pdam\_00022018).

The “black” module (*n*=1317 genes) was positively correlated with final F<sub>v</sub>/F<sub>m</sub> values and was not enriched for any KOG terms but was enriched for the BP GO terms “positive regulation of lipid metabolic process,” “negative regulation of growth” and “regulation of phosphatidylinositol 3-kinase signaling” with the module hub gene, the transcription factor protein c-FOS (pdam\_00011993, Table S9). The “royalblue” module (*n*=62 genes) was also positively correlated with final F<sub>v</sub>/F<sub>m</sub> values and had no significantly enriched KOG or GO terms (Figure 5).

The “lightcyan” module (*n*=98 genes) was negatively correlated with final F<sub>v</sub>/F<sub>m</sub> and MO<sub>2</sub> values and was enriched for the KOG term “extracellular structures” despite having no enriched GO terms and the module hub gene was similar to an *Acropora millepora* skeletal

matrix protein (pdam\_00023883, Table S9). The “darkgrey” module ( $n=131$  genes) was also negatively correlated with final  $F_v/F_m$  and  $MO_2$  values but had no enriched KOG or GO terms and an unknown hub gene (Figure 5, Table S9).

## 4 | DISCUSSION

In this study, we show that antibiotics treatments alter *Pocillopora* coral-associated bacterial communities by selectively reducing bacteria diversity, which is linked to reduced holobiont oxygen consumption, increased expression of coral immune response genes and decreased expression of cellular housekeeping and symbiosis maintenance genes. There was no significant difference in *Symbiodiniaceae* photochemical efficiency between control and antibiotics-treated samples (Figure 2a), indicating that the antibiotics used here do not impair *Symbiodiniaceae* photosynthetic machinery, contrary to previous studies (Gilbert et al., 2012; Soffer et al., 2008). In contrast, we hypothesize that the significant reduction in microfragment  $MO_2$  values in the antibiotics treatment was due to the direct killing, elimination and/or metabolic suppression of susceptible coral-associated bacteria (Figure 2b). Antibiotics treatment may also have directly affected coral host and *Symbiodiniaceae* respiration to diminish overall holobiont  $MO_2$  rates. Overall, our results suggest that antibiotics can cause a decrease in coral holobiont health by depleting beneficial microbes and/or suppressing holobiont metabolism, which allows a few persistent microbes to flourish in a potentially dysbiotic state and trigger costly host immune responses.

### 4.1 | Antibiotics treatments selectively alter coral-associated bacterial communities by reducing overall community diversity and dissimilarity

The *Pocillopora* corals that were examined in this study belong to two species across divergent mitochondrial lineages, host different dominant *Symbiodiniaceae* genera and were collected from environments with different thermal regimes in Panama. However, there was no significant effect of coral colony, mitochondrial lineage or source location on bacterial community composition and communities were similar across baseline and control samples (Figure 3a). This may be because all colonies were cultured together in a common-garden aquarium at the University of Miami for 5–16 years after collection. As expected, a 5-day treatment with the broad-spectrum antibiotics ampicillin, streptomycin and ciprofloxacin in filter-sterile seawater significantly altered bacterial community composition and reduced community diversity (Figure 3), similar to previous studies that have used antibiotics to alter coral microbiomes (Connelly et al., 2022; Glasl et al., 2016; Sweet et al., 2011, 2014). These changes were driven by the near elimination of ASVs in the families *Nitrincolaceae*, *Rhodobacteraceae* and *Alteromonadaceae*, among others, that were highly prevalent in baseline and control samples but reduced in antibiotics-treated samples (Figure 3d, Figure S8).

These “antibiotics-susceptible” core bacteria included representatives from the family *Rhodobacteraceae* and genera *Neptuniibacter* and *Kordiimonas* and each may have important functions within the coral holobiont.

For example, *Pocillopora*-associated *Rhodobacteraceae* have been implicated in nitrogen fixation, amino acid biosynthesis and sulphur metabolism (Geissler et al., 2021; Li et al., 2022; Meunier et al., 2021). Genomic evidence suggests that *Pocillopora* corals cannot synthesize eight essential amino acids, including the branched-chain amino acids isoleucine, leucine and valine and the sulphur-containing amino acid methionine (Cunning et al., 2018; Li et al., 2022), so the downregulation of branched-chain amino acid transport and sulphur compound catabolic process genes in antibiotics-treated corals suggests that *Rhodobacteraceae* may have important roles in supporting these metabolic exchanges (Figure 4c, Table S8). Similarly, bacteria in the genus *Neptuniibacter* (family *Nitrincolaceae*) associate with diverse marine organisms including corals, medusozoans and ascidians, where they have been hypothesized to provide various health benefits such as stimulation of growth and development (Fragoso Ados Santos et al., 2015; Keller et al., 2021; Schreiber et al., 2016). Bacteria in the genus *Kordiimonas* have also been detected in general association with *Pocillopora* corals, anemones and ascidians (Blasiak et al., 2014; Cahill et al., 2016; Zhang et al., 2021), however, specific functional roles have yet to be identified.

While antibiotics treatment was successful in reducing bacterial community diversity and eliminating many transiently associated and presumably antibiotics-susceptible bacteria, not all core bacteria were eliminated and several ASVs were observed to increase in relative abundance (Figure 3d, Table S6), despite the caveat that 16S rRNA gene amplicon sequencing data cannot distinguish whether these bacteria are still alive and metabolically active. These persistent ASVs included a single *Vibrio* ASV with 100% sequence similarity to the known coral pathogen *V. harveyi*, which could be driving the observed activation of coral immune responses through niche expansion and opportunistic infection following initial resistance to antibiotics (Luna et al., 2010; Meyer et al., 2015; Smith et al., 2015). Indeed, cultured *Vibrio* bacteria from *Pocillopora* corals have been shown to possess genomes encoding antibiotic resistance genes, virulence factors and quorum-sensing inhibitors (Li et al., 2022; Ma et al., 2018), indicating the potential for pathogenesis following microbiome disruption. Three *Micavibronaceae* ASVs also increased in relative abundance in antibiotics treatment samples and because *Micavibronaceae* have been documented to increase during heat stress in *Pocillopora* corals and sea sponges, this suggests their role as another group of opportunistic microbes (Li et al., 2021; Posadas et al., 2022).

Additionally, out of a total of seven unique *Endozooicomonas* ASVs detected in the dataset, a single *Endozooicomonas* ASV was identified in the core microbiome across all colonies and persisted and increased in relative abundance in antibiotics treatment samples. Bacteria in the genus *Endozooicomonas* are among the most conspicuous endosymbionts of *Pocillopora* corals, having been identified as core taxa across numerous studies throughout the genus' range,

living in multicellular aggregates within coral gastrodermal tissues and being vertically transmitted between generations in maternal oocytes (Damjanovic et al., 2020; Hernández-Zulueta et al., 2016; Neave et al., 2017). *Endozoicomonas* bacteria have been shown to resist the effects of nutrient enrichment and temperature stress in *P. verrucosa* from the Red Sea (Pogoreutz et al., 2018) and ampicillin and streptomycin antibiotics treatment in *P. acuta* and *P. damicornis* from Taiwan (Connelly et al., 2022), indicating an ability to persist in coral tissues under various disturbances. In other corals, *Endozoicomonas* bacteria have been shown to metabolize dimethylsulfoniopropionate (DMSP) and upregulate host cell attachment proteins and vitamin B biosynthesis processes following exposure to holobiont cues (Pogoreutz et al., 2022; Tandon et al., 2020). Future research should seek to characterize the genomic diversity, metabolic capacity and cellular niches of *Pocillopora*-associated *Endozoicomonas* bacteria to better understand the nature of this important symbiotic relationship.

Another persistent core ASVs belonging to the genus *Thalassospira*, which have been documented in symbiosis with corals, medusozoans and ascidians, are detected in seawater after *P. damicornis* spawning and produce a wide variety of secondary metabolites including the immunosuppressive thalassospiramides A, D and G (Blasiak et al., 2014; Ceh, van Keulen, et al., 2013; Um et al., 2013). A single ASV in the family *Arcobacteraceae* also persisted after antibiotics treatment and these bacteria are found in association with corals, cuttlefish and sea urchins and are capable of thiosulfate oxidation and production of fibronectin-binding proteins for host cell attachment (Li et al., 2022). Together, these bacteria should be investigated for their ability to persist within coral host tissues during targeted disturbances and assessed for their metabolic ability to contribute to holobiont nutrient exchanges and mediate–immune system crosstalk.

Other notable bacteria that were observed to persist in antibiotics-treated samples have been recently documented in intimate associations with cultured and in hospite *Symbiodiniaceae*. Bacteria in group SM1A02 (family *Phycisphaeraceae*) are commonly documented in the core microbiome of multiple-cultured *Symbiodiniaceae* genera (Camp et al., 2020; Lawson et al., 2018) and recorded in association with the dinoflagellate *Gambierdiscus* where they were shown to possess the genomic capacity for nitrogen and sulphur cycling and B-vitamin synthesis (Rambo et al., 2020). These bacteria have been barely studied and could represent new taxa to target for culturing, metabolic characterization and formal description, as well as understanding their role in coral–*Symbiodiniaceae* relationships.

#### 4.2 | Antibiotic bacterial community suppression activates coral immunity and stress response gene expression

*Pocillopora* transcriptome patterns showed strong colony variation. However, co-expression network analysis and functional

enrichment tests revealed that antibiotic bacterial community suppression is correlated with enhanced expression of coral immunity, inflammation and stress response genes at the expense of cellular housekeeping functions such as DNA replication, energy production, translation and cytoskeleton maintenance (Figures 4 and 5). Specifically, the positive correlation of the “lightyellow” and “orange” modules and negative correlation of the “brown” module with the antibiotics treatment indicate the existence of trade-offs between the activation of cellular immune responses, such as interleukin signalling pathways and coagulation cascades (Poole & Weis, 2014) and cellular housekeeping functions, such as ATP production and cytoskeleton maintenance (Figures 4c,d and 5). These changes may be related to the increased relative abundance of opportunistic microbes such as *Vibrio* bacteria in the coral holobiont following antibiotics treatment (Figure 3d) because these bacteria are known coral pathogens (Ben-Haim et al., 2003; Luna et al., 2010) that may possess antibiotics resistance genes and could shift to a pathogenic lifestyle following antibiotic disruption of the healthy community (Gao et al., 2021; Meyer et al., 2015; Smith et al., 2015). Prior studies implicated *Alteromonas* and *Vibrio* bacteria in driving dysbiosis following antibiotics treatment and heat stress in *P. acuta* and *P. damicornis* corals from Taiwan (Connelly et al., 2022) and while *Alteromonas* bacteria were reduced following the addition of ciprofloxacin in this study, several of the same key immune genes, including endoribonuclease ZC3H12B (pdam\_00012426), ETS-related transcription factor Elf-4 (pdam\_00016137) and ETS domain-containing protein Elk-1 (pdam\_00003296), were upregulated following antibiotics treatment (Table S7). Future studies should aim to characterize the prevalence and diversity of coral-associated bacteria that possess antibiotic-resistance genes and virulence factors and determine the immune mechanisms that allow healthy corals to resist infection to better understand the potential for breakout infections following environmental disturbances.

#### 4.3 | Antibiotics treatments as a practical tool for coral microbiome manipulation studies

Our experiment reveals the utility of antibiotics as an experimental tool for coral microbiome manipulation studies, as we succeeded in reducing the diversity of *Pocillopora* coral-associated bacteria by approximately 60% in only 5 days using a combination of broad-spectrum antibiotics in filter-sterile seawater. The persistence of potentially antibiotics-resistant and internally associated bacteria highlights the difficulty in obtaining truly germ-free corals for future experiments, as many of these bacteria are opportunistic pathogens, key mutualists with beneficial functions that support the health of the coral holobiont or have other context-dependent symbiotic roles. Additionally, our experiment cannot attribute the observed responses to antibiotics treatment to depletion of the native microbiota, persistence of antibiotic-resistant microbes or possible direct effects on host tissues (Morgan et al., 2016) and future research is required to determine the relative impact of these different factors.

Nonetheless, antibiotics treatments are promising tools for manipulating coral bacterial communities and identifying which of these holobiont functions (e.g. nutrient cycling, amino acid and vitamin synthesis, pathogen resistance, heat tolerance, etc.) are negatively impacted by a diminished microbiota (Domin et al., 2018; Fraune et al., 2015; Klimovich et al., 2020; Murillo-Rincon et al., 2017; Weiland-Bräuer et al., 2020). Experiments that use antibiotics followed by subsequent “recovery” treatments will yield insights into whether bacterial communities can be returned to healthy states by re-introduction of beneficial microbes (Assis et al., 2020; Damjanovic et al., 2019; Rosado et al., 2018; Santoro et al., 2021) and measuring the resulting holobiont phenotypes with integrative omics methods will reveal the genetic and molecular basis of coral-holobiont interactions in unprecedented detail.

## AUTHOR CONTRIBUTIONS

MTC and NTK conceived and designed the research, ACB provided experimental animals and equipment for physiology measurements, PRG supported experimental animal husbandry and gave technical advice on aquarium incubator setup, MTC and GS conducted the experiments and obtained physiological data and microscope images and AMPC helped with *Pocillopora* holobiont characterization and physiology data analysis. MTC analysed all physiology and sequencing datasets and wrote the first draft of the manuscript. All authors helped interpret the results and edited the final manuscript.

## ACKNOWLEDGEMENTS

We would like to thank Dr. Stephanie Rosales for bioinformatics assistance and NOAA's Ocean Chemistry and Ecosystems Division for the provision of the optical respirometer. This research was supported by the 2019 RSMAS David Rowland Fellowship awarded to MTC and by National Science Foundation Award #1951826 awarded to NTK.

## CONFLICT OF INTEREST STATEMENT

The authors declare no conflict of interest.

## DATA AVAILABILITY STATEMENT

Raw 16S rDNA gene amplicon reads and RNAseq reads were deposited into the NCBI Sequence Read Archive (SRA) under BioProject accession PRJNA818888. All the scripts used in the 16S and RNAseq data analysis are available on GitHub: [https://github.com/michaelconnelly/coral\\_antibiotics\\_physiology](https://github.com/michaelconnelly/coral_antibiotics_physiology).

## BENEFIT-SHARING STATEMENT

Benefits from this research accrue from sharing data, analysis scripts and results on public databases (described above) and this research addresses priority concerns in advancing coral conservation. More broadly, our group is committed to equitable international scientific partnerships and institutional capacity building.

## ORCID

Michael T. Connelly  <https://orcid.org/0000-0002-2084-4222>

Grace Snyder  <https://orcid.org/0003-3756-8540>

Ana M. Palacio-Castro  <https://orcid.org/0000-0002-0821-0286>  
Phillip R. Gillette  <https://orcid.org/0000-0001-9567-6908>  
Andrew C. Baker  <https://orcid.org/0000-0002-7866-2587>  
Nikki Taylor-Knowles  <https://orcid.org/0000-0002-4906-4537>

## REFERENCES

- Ainsworth, T. D., Krause, L., Bridge, T., Torda, G., Raina, J. B., Zakrzewski, M., Gates, R. D., Padilla-Gamiño, J. L., Spalding, H. L., Smith, C., Woolsey, E. S., Bourne, D. G., Bongaerts, P., Hoegh-Guldberg, O., & Leggat, W. (2015). The coral core microbiome identifies rare bacterial taxa as ubiquitous endosymbionts. *The ISME Journal*, 9(10), 2261–2274. <https://doi.org/10.1038/ismej.2015.39>
- Anderson, M. J. (2017). Permutational Multivariate Analysis of Variance (PERMANOVA). *Wiley StatsRef: Statistics Reference Online*, 1–15. <https://doi.org/10.1002/9781118445112.stat07841>
- Apprill, A., Marlow, H. Q., Martindale, M. Q., & Rappé, M. S. (2009). The onset of microbial associations in the coral *Pocillopora meandrina*. *The ISME Journal*, 3(6), 685–699. <https://doi.org/10.1038/ismej.2009.3>
- Apprill, A., McNally, S., Parsons, R., & Weber, L. (2015). Minor revision to V4 region SSU rRNA 806R gene primer greatly increases detection of SAR11 bacterioplankton. *Aquatic Microbial Ecology*, 75(2), 129–137. <https://doi.org/10.3354/ame01753>
- Assis, J. M., Villela, H., Abreu, F., Duarte, G., Roj, L., & Peixoto, R. (2020). Delivering Beneficial Microorganisms for Corals (BMCs): Rotifers as carriers of coral probiotics. *Frontiers in Microbiology*, 11, 608506. <https://doi.org/10.3389/fmicb.2020.608506>
- Barfield, S. J., Aglyamova, G. V., Bay, L. K., & Matz, M. V. (2018). Contrasting effects of *Symbiodinium* identity on coral host transcriptional profiles across latitudes. *Molecular Ecology*, 27(15), 3103–3115. <https://doi.org/10.1111/mec.14774>
- Ben-Haim, Y., Zicherman-Keren, M., & Rosenberg, E. (2003). Temperature-regulated bleaching and lysis of the Coral *Pocillopora damicornis* by the novel pathogen *Vibrio coralliilyticus*. *Applied and Environmental Microbiology*, 69(7), 4236–4242. <https://doi.org/10.1128/AEM.69.7.4236-4242.2003>
- Blasiak, L. C., Zinder, S. H., Buckley, D. H., & Hill, R. T. (2014). Bacterial diversity associated with the tunic of the model chordate *Ciona intestinalis*. *The ISME Journal*, 8(2), 309–320. <https://doi.org/10.1038/ismej.2013.156>
- Bokulich, N. A., Kaehler, B. D., Rideout, J. R., Dillon, M., Bolyen, E., Knight, R., Huttley, G. A., & Caporaso, G. (2018). Optimizing taxonomic classification of marker-gene amplicon sequences with QIIME 2's q2-feature-classifier plugin. *Microbiome*, 6, 90. <https://doi.org/10.1186/s40168-018-0470-z>
- Bosch, T. C. G., Guillemin, K., & McFall-Ngai, M. (2019). Evolutionary “experiments” in symbiosis: The Study of model animals provides insights into the mechanisms underlying the diversity of host-microbe interactions. *BioEssays*, 41(10), e1800256. <https://doi.org/10.1002/bies.201800256>
- Bourne, D. G., & Munn, C. B. (2005). Diversity of bacteria associated with the coral *Pocillopora damicornis* from the Great Barrier Reef. *Environmental Microbiology*, 7(8), 1162–1174. <https://doi.org/10.1111/j.1462-2920.2005.00793.x>
- Brener-Raffali, K., Clerissi, C., Vidal-Dupiol, J., Adjeroud, M., Bonhomme, F., Pratlong, M., Aurelle, D., Mitta, G., & Toulza, E. (2018). Thermal regime and host clade, rather than geography, drive *Symbiodinium* and bacterial assemblages in the scleractinian coral *Pocillopora damicornis sensu lato*. *Microbiome*, 6(1), 39. <https://doi.org/10.1186/s40168-018-0423-6>
- Cahill, P. L., Fidler, A. E., Hopkins, G. A., & Wood, S. A. (2016). Geographically conserved microbiomes of four temperate water tunnates. *Environmental Microbiology Reports*, 8(4), 470–478. <https://doi.org/10.1111/1758-2229.12391>

- Callahan, B. J., McMurdie, P. J., Rosen, M. J., Han, A. W., Johnson, A. J. A., & Holmes, S. P. (2016). DADA2: High resolution sample inference from Illumina amplicon data. *Nature Methods*, 13(7), 581–583. <https://doi.org/10.1038/nmeth.3869>
- Camp, E. F., Kahlike, T., Nitschke, M. R., Varkey, D., Fisher, N. L., Fujise, L., Goyen, S., Hughes, D. J., Lawson, C. A., Ros, M., Woodcock, S., Xiao, K., Leggat, W., & Suggett, D. J. (2020). Revealing changes in the microbiome of Symbiodiniaceae under thermal stress. *Environmental Microbiology*, 22(4), 1294–1309. <https://doi.org/10.1111/1462-2920.14935>
- Ceh, J., Kilburn, M. R., Cliff, J. B., Raina, J. B., van Keulen, M., & Bourne, D. G. (2013). Nutrient cycling in early coral life stages: *Pocillopora damicornis* larvae provide their algal symbiont (*Symbiodinium*) with nitrogen acquired from bacterial associates. *Ecology and Evolution*, 3(8), 2393–2400. <https://doi.org/10.1002/ece3.642>
- Ceh, J., van Keulen, M., & Bourne, D. G. (2011). Coral-associated bacterial communities on Ningaloo Reef, Western Australia. *FEMS Microbiology Ecology*, 75(1), 134–144. <https://doi.org/10.1111/j.1574-6941.2010.00986.x>
- Ceh, J., van Keulen, M., & Bourne, D. G. (2013). Intergenerational transfer of specific bacteria in corals and possible implications for offspring fitness. *Microbial Ecology*, 65(1), 227–231. <https://doi.org/10.1007/s00248-012-0105-z>
- Chevrette, M. G., Bratburd, J. R., Currie, C. R., & Stubbendieck, R. M. (2019). Experimental microbiomes: Models not to scale. *mSystems*, 4(4), e00175–19. <https://doi.org/10.1128/msystems.00175-19>
- Connelly, M. T., McRae, C. J., Liu, P. J., Martin, C. E., & Traylor-Knowles, N. (2022). Antibiotics alter *Pocillopora* coral-Symbiodiniaceae-bacteria interactions and cause microbial dysbiosis during heat stress. *Frontiers in Marine Science*, 8, 814124. <https://doi.org/10.3389/fmars.2021.814124>
- Cunning, R., Bay, R. A., Gillette, P., Baker, A. C., & Traylor-Knowles, N. (2018). Comparative analysis of the *Pocillopora damicornis* genome highlights role of immune system in coral evolution. *Scientific Reports*, 8(1), 16134. <https://doi.org/10.1038/s41598-018-34458>
- Damjanovic, K., Menéndez, P., Blackall, L. L., & van Oppen, M. J. H. (2020). Mixed-mode bacterial transmission in the common brooding coral *Pocillopora acuta*. *Environmental Microbiology*, 22(1), 397–412. <https://doi.org/10.1111/1462-2920.14856>
- Damjanovic, K., van Oppen, M. J. H., Menéndez, P., & Blackall, L. L. (2019). Experimental inoculation of coral recruits with marine bacteria indicates scope for microbiome manipulation in *Acropora tenuis* and *Platygyra daedalea*. *Frontiers in Microbiology*, 10, 1702. <https://doi.org/10.3389/fmicb.2019.01702>
- Davis, N. M., Proctor, D. M., Holmes, S. P., Relman, D. A., & Callahan, B. J. (2017). Simple statistical identification and removal of contaminant sequences in marker-gene and metagenomics data. *Microbiome*, 6(1), 226. <https://doi.org/10.1101/221499>
- Dobin, A., Davis, C. A., Schlesinger, F., Drenkow, J., Zaleski, C., Jha, S., Batut, P., Chaisson, M., & Gingeras, T. R. (2013). STAR: Ultrafast universal RNA-seq aligner. *Bioinformatics*, 29(1), 15–21. <https://doi.org/10.1093/bioinformatics/bts635>
- Dobson, A. J., Chaston, J. M., & Douglas, A. E. (2016). The *Drosophila* transcriptional network is structured by microbiota. *BMC Genomics*, 17(1), 975. <https://doi.org/10.1186/s12864-016-3307-9>
- Domin, H., Zurita-Gutiérrez, Y. H., Scotti, M., Buttlar, J., Humeida, U. H., & Fraune, S. (2018). Predicted bacterial interactions affect in vivo microbial colonization dynamics in *Nematostella*. *Frontiers in Microbiology*, 9, 728. <https://doi.org/10.3389/fmicb.2018.00728>
- Drown, M. K., DeLiberto, A. N., Crawford, D. L., & Oleksiak, M. F. (2020). An innovative setup for high-throughput respirometry of small aquatic animals. *Frontiers in Marine Science*, 7, 581104. <https://doi.org/10.3389/fmars.2020.581104>
- Edgar, R. C. (2004). MUSCLE: Multiple sequence alignment with high accuracy and high throughput. *Nucleic Acids Research*, 32(5), 1792–1797. <https://doi.org/10.1093/nar/gkh340>
- Epstein, H. E., Torda, G., & van Oppen, M. J. H. (2019). Relative stability of the *Pocillopora acuta* microbiome throughout a thermal stress event. *Coral Reefs*, 38, 373–386. <https://doi.org/10.1007/s00338-019-01783-y>
- Flot, J. F., Magalon, H., Cruaud, C., Couloux, A., & Tillier, S. (2008). Patterns of genetic structure among Hawaiian corals of the genus *Pocillopora* yield clusters of individuals that are compatible with morphology. *Comptes Rendus Biologies*, 331(3), 239–247. <https://doi.org/10.1016/j.crvi.2007.12.003>
- Flot, J. F., & Tillier, S. (2007). The mitochondrial genome of *Pocillopora* (Cnidaria: Scleractinia) contains two variable regions: The putative D-loop and a novel ORF of unknown function. *Gene*, 401(1–2), 80–87. <https://doi.org/10.1016/j.gene.2007.07.006>
- Fragoso Ados Santos, H., Duarte, G. A., Rachid, C. T., Chaloub, R. M., Calderon, E. N., Marangoni, L. F., Bianchini, A., Nudi, A. H., do Carmo, F. L., van Elsas, J. D., Rosado, A. S., Castro, C. B., & Peixoto, R. S. (2015). Impact of oil spills on coral reefs can be reduced by bioremediation using probiotic microbiota. *Scientific Reports*, 5, 18268. <https://doi.org/10.1038/srep18268>
- Fraune, S., Anton-Erxleben, F., Augustin, R., Franzenburg, S., Knop, M., Schröder, K., Willoweit-ohl, D., & Bosch, T. C. G. (2015). Bacteria-bacteria interactions within the microbiota of the ancestral metazoan Hydra contribute to fungal resistance. *The ISME Journal*, 9(7), 1543–1556. <https://doi.org/10.1038/ismej.2014.239>
- Gao, C., Garren, M., Penn, K., Fernandez, V. I., Seymour, J. R., Thompson, J. R., Raina, J. B., & Stocker, R. (2021). Coral mucus rapidly induces chemokinesis and genome-wide transcriptional shifts toward early pathogenesis in a bacterial coral pathogen. *The ISME Journal*, 15, 3668–3682. <https://doi.org/10.1038/s41396-021-01024-7>
- Geissler, L., Meunier, V., Rädecker, N., Perna, G., Rodolfo-Metalpa, R., Houlbrèque, F., & Voolstra, C. R. (2021). Highly variable and non-complex diazotroph communities in corals from ambient and high CO<sub>2</sub> environments. *Frontiers in Marine Science*, 8, 754682. <https://doi.org/10.3389/fmars.2021.754682>
- Gélin, P., Postaire, B., Fauvelot, C., & Magalon, H. (2017). Reevaluating species number, distribution and endemism of the coral genus *Pocillopora* Lamarck, 1816 using species delimitation methods and microsatellites. *Molecular Phylogenetics and Evolution*, 109, 430–446. <https://doi.org/10.1016/j.ympev.2017.01.018>
- Gibbin, E., Gavish, A., Krueger, T., Kramarsky-Winter, E., Shapiro, O., Guiet, R., Jensen, L., Vardi, A., & Meibom, A. (2018). *Vibrio corrallilyticus* infection triggers a behavioural response and perturbs nutritional exchange and tissue integrity in a symbiotic coral. *The ISME Journal*, 13, 989–1003. <https://doi.org/10.1038/s41396-018-0327-2>
- Gilbert, J. A., Jansson, J. K., & Knight, R. (2014). The Earth Microbiome project: Successes and aspirations. *BMC Biology*, 12(1), 69. <https://doi.org/10.1186/s12915-014-0069-1>
- Gilbert, J. A., Hill, R., Doblin, M. A., & Ralph, P. J. (2012). Microbial consortia increase thermal tolerance of corals. *Marine Biology*, 159(8), 1763–1771. <https://doi.org/10.1007/s00227-012-1967-9>
- Glasl, B., Herndl, G. J., & Frade, P. R. (2016). The microbiome of coral surface mucus has a key role in mediating holobiont health and survival upon disturbance. *The ISME Journal*, 10(9), 2280–2292. <https://doi.org/10.1038/ismej.2016.9>
- Gloor, G. B., Macklaim, J. M., Pawlowsky-Glahn, V., & Egoscue, J. J. (2017). Microbiome datasets are compositional: And this is not optional. *Frontiers in Microbiology*, 8, 2224. <https://doi.org/10.3389/fmicb.2017.02224>
- Harianto, J., Carey, N., & Byrne, M. (2019). respR—An R package for the manipulation and analysis of respirometry data. *Methods in Ecology and Evolution*, 10, 912–920. <https://doi.org/10.1111/2041-210x.13162>
- Hernández-Zulueta, J., Araya, R., Vargas-Ponce, O., Díaz-Pérez, L., Rodríguez-Troncoso, A. P., Ceh, J., Ríos-Jara, E., & Rodríguez-Zaragoza, F. A. (2016). First deep screening of bacterial assemblages associated with corals of the Tropical Eastern Pacific. *FEMS Microbiology Ecology*, 100(10), 1–10. <https://doi.org/10.1093/femsre/fsw060>

- Microbiology Ecology, 92(12), fiw196. <https://doi.org/10.1093/femsec-fiw196>
- Hoffman, G. E., & Schadt, E. E. (2016). variancePartition: Interpreting drivers of variation in complex gene expression studies. *BMC Bioinformatics*, 17(1), 17–22. <https://doi.org/10.1186/s12859-016-1323-z>
- Katoh, K., & Standley, D. M. (2013). MAFFT multiple sequence alignment software version 7: Improvements in performance and usability. *Molecular Biology and Evolution*, 30(4), 772–780. <https://doi.org/10.1093/molbev/mst010>
- Keller, A. G., Apprill, A., Lebaron, P., Robbins, J., Romano, T. A., Overton, E., Rong, Y., Yuan, R., Pollara, S., & Whalen, K. E. (2021). Characterizing the culturable surface microbiomes of diverse marine animals. *FEMS Microbiology Ecology*, 97(4), fiab040. <https://doi.org/10.1093/femsec/fiab040>
- Klimovich, A., Giacomello, S., Björklund, Å., Faure, L., Kaucka, M., Giez, C., Murillo-Rincon, A. P., Matt, A. S., Willoweit-Ohl, D., Crupi, G., de Anda, J., Wong, G. C. L., D'Amato, M., Adameyko, I., & Bosch, T. C. G. (2020). Prototypical pacemaker neurons interact with the resident microbiota. *Proceedings of the National Academy of Sciences of the United States of America*, 117, 17854–17863. <https://doi.org/10.1073/pnas.1920469117>
- Kostic, A. D., Howitt, M. R., & Garrett, W. S. (2013). Exploring host-microbiota interactions in animal models and humans. *Genes and Development*, 27(7), 701–718. <https://doi.org/10.1101/gad.212522.112>
- Lahti, L., & Shetty, S. (2019). *microbiome R package*.
- Langfelder, P., & Horvath, S. (2008). WGCNA: An R package for weighted correlation network analysis. *BMC Bioinformatics*, 9, 559. <https://doi.org/10.1186/1471-2105-9-559>
- Lawson, C. A., Raina, J. B., Kahlke, T., Seymour, J. R., & Suggett, D. J. (2018). Defining the core microbiome of the symbiotic dinoflagellate *Symbiodinium*. *Environmental Microbiology Reports*, 10(1), 7–11. <https://doi.org/10.1111/1758-2229.12599>
- Lema, K. A., Willis, B. L., & Bourne, D. G. (2012). Corals form characteristic associations with symbiotic nitrogen-fixing bacteria. *Applied and Environmental Microbiology*, 78(9), 3136–3144. <https://doi.org/10.1128/AEM.07800-11>
- Li, J., Long, L., Zou, Y., & Zhang, S. (2021). Microbial community and transcriptional responses to increased temperatures in coral *Pocillopora damicornis* holobiont. *Environmental Microbiology*, 23(2), 826–843. <https://doi.org/10.1111/1462-2920.15168>
- Li, J., Zou, Y., Yang, J., Li, Q., Bourne, D. G., Sweet, M., Liu, C., Guo, A., & Zhang, S. (2022). Cultured bacteria provide insight into the functional potential of the coral-associated microbiome. *mSystems*, 7(4), e0032722.
- Liao, Y., Smyth, G. K., & Shi, W. (2014). featureCounts: An efficient general purpose program for assigning sequence reads to genomic features. *Bioinformatics*, 30(7), 923–930. <https://doi.org/10.1093/bioinformatics/btt656>
- Liu, H., Stephens, T. G., González-Pech, R. A., Beltran, V. H., Lapeyre, B., Bongaerts, P., Cooke, I., Aranda, M., Bourne, D. G., Forêt, S., Miller, D. J., van Oppen, M. J. H., Voolstra, C. R., Ragan, M. A., & Chan, C. X. (2018). *Symbiodinium* genomes reveal adaptive evolution of functions related to coral-dinoflagellate symbiosis. *Communications Biology*, 1, 95. <https://doi.org/10.1038/s42003-018-0098-3>
- Love, M. I., Huber, W., & Anders, S. (2014). Moderated estimation of fold change and dispersion for RNA-seq data with DESeq2. *Genome Biology*, 15(12), 550. <https://doi.org/10.1186/s13059-014-0550-8>
- Luna, G. M., Bongiorni, L., Gili, C., Biavasco, F., & Danovaro, R. (2010). *Vibrio harveyi* as a causative agent of the White Syndrome in tropical stony corals. *Environmental Microbiology Reports*, 2(1), 120–127. <https://doi.org/10.1111/j.1758-2229.2009.00114.x>
- Ma, Z. P., Song, Y., Cai, Z. H., Lin, Z. J., Lin, G. H., Wang, Y., & Zhou, J. (2018). Anti-quorum sensing activities of selected coral symbiotic bacterial extracts from the South China Sea. *Frontiers in Cellular and Infection Microbiology*, 8, 144. <https://doi.org/10.3389/fcimb.2018.00144>
- Marotz, C., Sharma, A., Humphrey, G., Gottel, N., Daum, C., Gilbert, J. A., Eloë-Fadrosh, E., & Knight, R. (2019). Triplicate PCR reactions for 16S rRNA gene amplicon sequencing are unnecessary. *BioTechniques*, 67(1), 29–32. <https://doi.org/10.2144/btn-2018-0192>
- Matz, M. V. (2019). KOGMWU: Functional Summary and Meta-Analysis of Gene Expression Data.
- McDonald, D., Clemente, J. C., Kuczynski, J., Rideout, J. R., Stombaugh, J., Wendel, D., Wilke, A., Huse, S., Hufnagle, J., Meyer, F., Knight, R., & Caporaso, G. (2012). The Biological Observation Matrix (BIOM) format or: How I learned to stop worrying and love the ome-ome. *GigaScience*, 464(1), 7. <https://doi.org/10.1186/2047-217X-1-7>
- McMurdie, P. J., & Holmes, S. (2013). phyloseq: An R package for reproducible interactive analysis and graphics of microbiome census data. *PLoS One*, 8(4), e61217. <https://doi.org/10.1371/journal.pone.0061217>
- Meunier, V., Geissler, L., Bonnet, S., Rädecker, N., Perna, G., Grossi, O., Lambert, C., Rodolfo-Metalpa, R., Voolstra, C. R., & Houlbrèque, F. (2021). Microbes support enhanced nitrogen requirements of coral holobionts in a high CO<sub>2</sub> environment. *Molecular Ecology*, 30(22), 5888–5899. <https://doi.org/10.1111/mec.16163>
- Meyer, J. L., Gunasekera, S. P., Scott, R. M., Paul, V. J., & Teplit斯基, M. (2015). Microbiome shifts and the inhibition of quorum sensing by Black Band Disease cyanobacteria. *The ISME Journal*, 10(5), 1204–1216. <https://doi.org/10.1038/ismej.2015.184>
- Morgun, A., Dzutsev, A., Xiaoxi, D., Greer, R. L., Sexton, D. J., Ravel, J., Schuster, M., Hsiao, W., Matzinger, P., & Shulzhenko, N. (2016). Uncovering effects of antibiotics on the host and microbiota using transkingdom gene networks. *Gut*, 64(11), 1732–1743. <https://doi.org/10.1136/gutjnl-2014-308820>. *Uncovering*
- Murillo-Rincon, A. P., Klimovich, A., Pemöller, E., Taubenheim, J., Mortzfeld, B., Augustin, R., & Bosch, T. C. G. (2017). Spontaneous body contractions are modulated by the microbiome of Hydra. *Scientific Reports*, 7(1), 15937. <https://doi.org/10.1038/s41598-017-16191-x>
- Neave, M. J., Rachmawati, R., Xun, L., Michell, C. T., Bourne, D. G., Apprill, A., & Voolstra, C. R. (2017). Differential specificity between closely related corals and abundant *Endozooicomonas* endosymbionts across global scales. *The ISME Journal*, 11(1), 186–200. <https://doi.org/10.1038/ismej.2016.95>
- Oksanen, J., Blanchet, F. G., Friendly, M., Kindt, R., Legendre, P., McGlinn, D., Minchin, P. R., O'Hara, R. B., Simpson, G. L., Solymos, P., Stevens, M. H. H., Szoecs, E., & Wagner, H. (2019). *vegan: Community ecology package*.
- Palarea-Albaladejo, J., & Martín-Fernández, J. A. (2015). zCompositions—R package for multivariate imputation of left-censored data under a compositional approach. *Chemometrics and Intelligent Laboratory Systems*, 143, 85–96. <https://doi.org/10.1016/j.chemolab.2015.02.019>
- Paradis, E. (2010). pegas: An R package for population genetics with an integrated-modular approach. *Bioinformatics*, 26(3), 419–420. <https://doi.org/10.1093/bioinformatics/btp696>
- Peixoto, R. S., Rosado, P. M., Leite, D. C., Rosado, A. S., & Bourne, D. G. (2017). Beneficial Microorganisms for Corals (BMC): Proposed mechanisms for coral health and resilience. *Frontiers in Microbiology*, 8, 341. <https://doi.org/10.3389/fmicb.2017.00341>
- Pinzón, J. H., Sampayo, E., Cox, E., Chauka, L. J., Chen, C. A., Voolstra, C. R., & Lajeunesse, T. C. (2013). Blind to morphology: Genetics identifies several widespread ecologically common species and few endemics among Indo-Pacific cauliflower corals (*Pocillopora*, *Scleractinia*). *Journal of Biogeography*, 40(8), 1595–1608. <https://doi.org/10.1111/jbi.12110>
- Pogoreutz, C., Oakley, C. A., Rädecker, N., Cárdenas, A., Perna, G., Xiang, N., Peng, L., Davy, S. K., Ngugi, D. K., & Voolstra, C. R. (2022).

- Coral holobiont cues prime *Endozoicomonas* for a symbiotic life-style. *The ISME Journal*, 16, 1883–1895. <https://doi.org/10.1038/s41396-022-01226-7>
- Pogoreutz, C., Rädecker, N., Cárdenas, A., Gärdes, A., Wild, C., & Voolstra, C. R. (2018). Dominance of *Endozoicomonas* bacteria throughout coral bleaching and mortality suggests structural inflexibility of the *Pocillopora verrucosa* microbiome. *Ecology and Evolution*, 8, 2240–2252. <https://doi.org/10.1002/ece3.3830>
- Poole, A. Z., & Weis, V. M. (2014). TIR-domain-containing protein repertoire of nine anthozoan species reveals coral-specific expansions and uncharacterized proteins. *Developmental and Comparative Immunology*, 46(2), 480–488. <https://doi.org/10.1016/j.dci.2014.06.002>
- Posadas, N., Baquiran, J. I. P., Nada, M. A. L., Kelly, M., & Conaco, C. (2022). Microbiome diversity and host immune functions influence survivorship of sponge holobionts under future ocean conditions. *The ISME Journal*, 16(1), 58–67. <https://doi.org/10.1038/s41396-021-01050-5>
- Price, M. N., Dehal, P. S., & Arkin, A. P. (2010). FastTree 2—approximately maximum-likelihood trees for large alignments. *PLoS One*, 5(3), e9490. <https://doi.org/10.1371/journal.pone.0009490>
- Quast, C., Pruesse, E., Yilmaz, P., Gerken, J., Schweer, T., Yarza, P., Peplies, J., & Glöckner, F. O. (2013). The SILVA ribosomal RNA gene database project: Improved data processing and web-based tools. *Nucleic Acids Research*, 41(D1), 590–596. <https://doi.org/10.1093/nar/gks1219>
- Rambo, I. M., Dombrowski, N., Constant, L., Erdner, D., & Baker, B. J. (2020). Metabolic relationships of uncultured bacteria associated with the microalgae *Gambierdiscus*. *Environmental Microbiology*, 22(5), 1764–1783. <https://doi.org/10.1111/1462-2920.14878>
- Risely, A. (2020). Applying the core microbiome to understand host-microbe systems. *Journal of Animal Ecology*, 89(7), 1549–1558. <https://doi.org/10.1111/1365-2656.13229>
- Rosado, P. M., Leite, D. C. A., Duarte, G. A. S., Chaloub, R. M., Jospin, G., Nunes da Rocha, U., P Saraiva, J., Dini-Andreote, F., Eisen, J. A., Bourne, D. G., & Peixoto, R. S. (2018). Marine probiotics: Increasing coral resistance to bleaching through microbiome manipulation. *The ISME Journal*, 13, 921–936. <https://doi.org/10.1038/s41396-018-0323-6>
- Santoro, E. P., Borges, R. M., Espinoza, J. L., Freire, M., Messias, C. S. M. A., Villela, H. D. M., Pereira, L. M., Vilela, C. L. S., Rosado, J. G., Cardoso, P. M., Rosado, P. M., Assis, J. M., Duarte, G. A. S., Perna, G., Rosado, A. S., Macrae, A., Dupont, C. L., Nelson, K. E., Sweet, M. J., ... Peixoto, R. S. (2021). Coral microbiome manipulation elicits metabolic and genetic restructuring to mitigate heat stress and evade mortality. *Science Advances*, 7(33), 19–21. <https://doi.org/10.1126/sciadv.abg3088>
- Schmidt-Roach, S., Miller, K. J., Lundgren, P., & Andreakis, N. (2014). With eyes wide open: A revision of species within and closely related to the *Pocillopora damicornis* species complex (Scleractinia; Pocilloporidae) using morphology and genetics. *Zoological Journal of the Linnean Society*, 170(1), 1–33. <https://doi.org/10.1111/zoj.12092>
- Schreiber, L., Kjeldsen, K. U., Funch, P., Jensen, J., Obst, M., López-Legentil, S., & Schramm, A. (2016). *Endozoicomonas* are specific, facultative symbionts of sea squirts. *Frontiers in Microbiology*, 7, 1042. <https://doi.org/10.3389/fmicb.2016.01042>
- Shoguchi, E., Beedessee, G., Hisata, K., Tada, I., Narisoko, H., Satoh, N., Kawachi, M., & Shinzato, C. (2021). A new dinoflagellate genome illuminates a conserved gene cluster involved in sunscreen biosynthesis. *Genome Biology and Evolution*, 13(2), evaa235. <https://doi.org/10.1093/gbe/evaa235>
- Smith, D., Leary, P., Craggs, J. R. K., Bythell, J. C., & Sweet, M. (2015). Microbial communities associated with healthy and white syndrome-affected *Echinopora lamellosa* in aquaria and experimental treatment with the antibiotic ampicillin. *PLoS One*, 10(3), e0121780. <https://doi.org/10.1371/journal.pone.0121780>
- Soffer, N., Gibbs, P. D. L., & Baker, A. C. (2008). Practical applications of contaminant-free *Symbiodinium* cultures grown on solid media. *Proceedings of the 11th International Coral Reef Symposium*, 5, 7–11.
- Song, Y., Cai, Z. H., Lao, Y. M., Jin, H., Ying, K. Z., Lin, G. H., & Zhou, J. (2018). Antibiofilm activity substances derived from coral symbiotic bacterial extract inhibit biofouling by the model strain *Pseudomonas aeruginosa* PAO1. *Microbial Biotechnology*, 11(6), 1090–1105. <https://doi.org/10.1111/1751-7915.13312>
- Sweet, M. J., Croquer, A., & Bythell, J. C. (2011). Dynamics of bacterial community development in the reef coral *Acropora muricata* following experimental antibiotic treatment. *Coral Reefs*, 30(4), 1121–1133. <https://doi.org/10.1007/s00338-011-0800-0>
- Sweet, M. J., Croquer, A., & Bythell, J. C. (2014). Experimental antibiotic treatment identifies potential pathogens of white band disease in the endangered Caribbean coral *Acropora cervicornis*. *Proceedings of the Royal Society B: Biological Sciences*, 281(1788), 20140094. <https://doi.org/10.1098/rspb.2014.0094>
- Tandon, K., Lu, C. Y., Chiang, P. W., Wada, N., Yang, S. H., Chan, Y. F., Chiou, Y. J., Chou, M. S., Chen, W. M., & Tang, S. L. (2020). Comparative genomics: Dominant coral-bacterium *Endozoicomonas acroporae* metabolizes dimethylsulfoniopropionate (DMSP). *The ISME Journal*, 14, 1290–1303. <https://doi.org/10.1038/s41396-020-0610-x>
- Um, S., Pyee, Y., Kim, E. H., Lee, S. K., Shin, J., & Oh, D. C. (2013). Thalassospiramide G, a new  $\gamma$ -amino-acid-bearing peptide from the marine bacterium *Thalassospira* sp. *Marine Drugs*, 11(3), 611–622. <https://doi.org/10.3390/md11030611>
- van Oppen, M. J. H., Bongaerts, P., Frade, P., Peplow, L. M., Boyd, S. E., Nim, H. T., & Bay, L. K. (2018). Adaptation to reef habitats through selection on the coral animal and its associated microbiome. *Molecular Ecology*, 27(14), 2956–2971. <https://doi.org/10.1111/mec.14763>
- Weiland-Bräuer, N., Pinnow, N., Langfeldt, D., Roik, A., Güllert, S., Chibani, C. M., Reusch, T. B. H., & Schmitz, R. A. (2020). The native microbiome is crucial for offspring generation and fitness of *Aurelia aurita*. *MBio*, 11(6), e02336–20. <https://doi.org/10.1128/mBio.02336-20>
- Wickham, H. (2016). *ggplot2: Elegant graphics for data analysis*. Springer-Verlag.
- Wickham, H., Averick, M., Bryan, J., Chang, W., McGowan, L. D., François, R., Grolemund, G., Hayes, A., Henry, L., Hester, J., Kuhn, M., Pedersen, T. L., Miller, E., Bache, S. M., Müller, K., Ooms, J., Robinson, D., Seidel, D. P., Spinu, V., ... Yutani, H. (2019). Welcome to the Tidyverse. *Journal of Open Source Software*, 4(43), 1686. <https://doi.org/10.21105/joss.01686>
- Wright, R. M., Kenkel, C. D., Dunn, C. E., Shilling, E. N., Bay, L. K., & Matz, M. V. (2017). Intraspecific differences in molecular stress responses and coral pathobiome contribute to mortality under bacterial challenge in *Acropora millepora*. *Scientific Reports*, 7(1), 2609. <https://doi.org/10.1038/s41598-017-02685-1>
- Xia, Y., & Sun, J. (2017). Hypothesis testing and statistical analysis of microbiome. *Genes and Diseases*, 4(3), 138–148. <https://doi.org/10.1016/j.gendis.2017.06.001>
- Zhang, Y., Yang, Q., Ling, J., Long, L., Huang, H., Yin, J., Wu, M., Tang, X., Lin, X., Zhang, Y., & Dong, J. (2021). Shifting the microbiome of a coral holobiont and improving host physiology by inoculation with a potentially beneficial bacterial consortium. *BMC Microbiology*, 21(1), 130. <https://doi.org/10.1186/s12866-021-02167-5>
- Zhou, Z., Zhao, S., Tang, J., Liu, Z., Wu, Y., Wang, Y., & Lin, S. (2019). Altered immune landscape and disrupted coral-symbiodinium symbiosis in the scleractinian coral *Pocillopora damicornis* by *Vibrio corallilyticus* challenge. *Frontiers in Physiology*, 10, 366. <https://doi.org/10.3389/fphys.2019.00366>

Ziegler, M., Grupstra, C. G. B., Barreto, M. M., Eaton, M., BaOmar, J., Zubier, K., Al-Sofyani, A., Turki, A. J., Ormond, R., & Voolstra, C. R. (2019). Coral bacterial community structure responds to environmental change in a host-specific manner. *Nature Communications*, 10(1), 3092. <https://doi.org/10.1038/s41467-019-10969-5>

#### SUPPORTING INFORMATION

Additional supporting information can be found online in the Supporting Information section at the end of this article.

**How to cite this article:** Connelly, M. T., Snyder, G., Palacio-Castro, A. M., Gillette, P. R., Baker, A. C., & Traylor-Knowles, N. (2023). Antibiotics reduce *Pocillopora* coral-associated bacteria diversity, decrease holobiont oxygen consumption and activate immune gene expression. *Molecular Ecology*, 00, 1–18. <https://doi.org/10.1111/mec.17049>